

Strong electrostatic interactions in spherical colloidal systems

René Messina*, Christian Holm†, and Kurt Kremer‡

Max-Planck-Institut für Polymerforschung, Ackermannweg 10, 55128, Mainz, Germany

(February 18, 2019)

Abstract

We investigate spherical macroions in the strong Coulomb coupling regime within the primitive model in salt-free environment. We first show that the ground state of every isolated colloid is naturally overcharged by simple electrostatic arguments illustrated by the Gillespie rule. We furthermore demonstrate that in the strong Coulomb coupling this mechanism leads to ionized states and thus to long range attractions between like-charged spheres. Furthermore we use molecular dynamics simulations to study in detail the counterion distribution for one and two highly charged colloids for the ground state as well as for finite temperatures. We compare our results in terms of a simple version of a Wigner crystal theory and find excellent qualitative and quantitative agreement.

PACS numbers: 82.70.Dd, 61.20.Qg, 41.20.-q

Typeset using REVTEX

*email: messina@mpip-mainz.mpg.de

†email: holm@mpip-mainz.mpg.de

‡email: k.kremer@mpip-mainz.mpg.de

I. INTRODUCTION

Charged colloidal suspensions are often encountered in the everyday life (technology, biology, medicine ...) and have an important practical impact [1]. In numerous application-oriented situations, electrostatic repulsion among colloids (macroions) is desired in order to obtain a stabilized suspension. Consequently the understanding of the electrostatic interaction in such systems is motivated by practical as well as theoretical interests. There is recent experimental evidence that the effective interaction between two like-charged spherical colloids (in the presence of neutralizing salts) can be attractive in the presence of one or two glass walls [2–4]. This is in contrast with the classical work of Derjaguin, Landau, Verwey and Overbeek (DLVO) based on a linearized Poisson Boltzmann theory [5,6], which foresees only repulsive effective Coulomb forces between two like-charged spheres even in confined geometry. There are some indications that this attraction might be explainable in terms of hydrodynamic effects induced by the walls [7].

Already in the bulk case there have been disputes for a long time about the existence of long range attractive forces, triggered mainly by the observation of voids in colloidal solutions [8–11]. There is no clear experimental and theoretical picture, either, and there have been speculations that the experiments observed phase coexistence. Recent theoretical [12–14] and simulation [15–18] investigations have shown the existence of *short range* attraction.

In two short communications [19,20], we demonstrated by molecular dynamics (MD) simulations, how a mechanism involving overcharged and undercharged spherical macroions could lead to a *strong long range* attraction between charged spheres. In this paper we give a more detailed account and elaborate on the physical mechanism responsible for *charge inversion* (overcharge). Why and how does a charged particle strongly “bind” electrostatically at its surface so many counterions that its net charge changes sign? We further will discuss the necessary ingredients to explain this phenomenon in terms of a simple Wigner crystal theory. Using this Ansatz we show that it is possible for a pair of colloids which are sufficiently different in charge density to have an ionized ground state. Both, the one

and two colloid cases, are treated in terms of analytical predictions and verifications by simulation. Of special interest are the energy barriers necessary to cross from a neutral pair to an ionized pair state. We finally demonstrate by explicit simulations that the described features survive also at finite temperature case.

The paper is organized as follows: in Sec. II a simple model based on the Gillespie rule is proposed to understand charge inversion. Section III contains details of our MD simulation model. Section IV is devoted for the study of a single highly charged colloid. In Sec. V we investigate the situation where two colloids are present. Finally, in Sec. VI we outline a summary of the results.

II. UNDERSTANDING OVERCHARGING VIA THE GILLESPIE RULE

Here we propose a simple model solely based on electrostatic energy considerations in order to understand the phenomenon of charge inversion for strongly coupled systems. Because of the analogy between a spherical macroion surrounded by counterions and an atom [i. e. nucleus + electrons], it turns out be fruitful to use classical pictures of atomic physics in order to gain comprehension of certain phenomena occurring in mesoscopic colloidal systems [19,20]. To study the possibility of overcharging a single macroion, we recall the Gillespie rule also known as the valence-shell electron-pair repulsion (VSEPR) theory [21–23] which is well known in chemistry to predict the molecular geometry in covalent compounds. Note that originally this model has nothing to do with overcharge. Applying simple electrostatics one can compute that the *ground state structure* of two, three, four and five electrons disposed on a hard sphere corresponds to simple geometrical situations like those depicted in Fig. 1). The electrons try to maximize their mutual distances which leads, for example, in the case of 3 and 4 electrons to equilateral triangular and tetrahedral arrangements.

Now, we can apply this concept to a spherical colloid of radius a , central charge $Z_m = +2e$, where e is the elementary charge, and N_c monovalent counterions. By referring to Fig. 1, the *neutral* system corresponds to the case where two counterions are present, and the

three other cases (three, four and five counterions) correspond to *non-neutral overcharged* states.

The total electrostatic energy $E(N_c)$ is merely made up of two terms: i) an attractive term $E_{att}(N_c)$ due to the attraction between the counterions and the central charge and ii) a repulsive term $E_{rep}(N_c)$ due to the repulsion among the counterions. The final expression for the electrostatic energy as a function of the number of counter ions reads

$$E(N_c) = E_{att}(N_c) + E_{rep}(N_c) = k_B T_0 \frac{l_B}{a} [-N_c Z_m + f(\theta)], \quad (1)$$

where $l_B = e^2 / (4\pi\epsilon_0\epsilon_r k_B T_0)$ is the Bjerrum length, $T_0 = 298K$ is the room temperature and $f(\theta)$ is the repulsive energy part which is solely a function of the *topology* (relative angles between counterions, such as α and β appearing in Fig. 1, which also depend on N_c) of the ground state figure. For the specific cases reported in Fig. 1, the calculation of $E(N_c)$, with $2 \leq N_c \leq 5$, is straightforward and the corresponding energy values are given in Fig. 1. One deduces that the maximally obtainable overcharging is $-2e$ (i. e. 100%) around the central charge. That is, the excess counterions gain more energy by assuming a topological favorable configuration than by escaping to infinity, the simple reason of overcharge. Note the arguments for overcharging are independent of the Bjerrum length and of the sphere radius, which enter only as prefactors in Eq. (1).

To safely use this above outlined model one has just to ensure that the counterion size is small enough to avoid excluded volume effects, which in practice is always true. The important message is that, from an energy point of view, a colloid *always* tends to be overcharged. Obviously, for high central charge, the direct computation of the electrostatic energy by using the exact equation (1) becomes extremely complicated. Therefore we resort to simulations for highly charged spheres.

III. SIMULATION MODEL

The system under consideration contains two types of spherical charges: (i) one or two macroion(s) with a bare central charge $Q = -Z_m e$ (with $Z_m > 0$) and (ii) small counterions

of diameter σ with charge $q = +Z_c e$ (with $Z_c = 2$) to neutralize the whole system. All these ions are confined in an impermeable cell and the macroion(s) is (are) held fixed.

The molecular dynamics (MD) technique employed here is similar to this used in previous studies [19,20]. In order to simulate a canonical ensemble, the motion of the counterions is coupled to a heat bath acting through a weak stochastic force $\mathbf{W}(t)$. The equation of motion of counterion i reads

$$m \frac{d^2 \mathbf{r}_i}{dt^2} = -\nabla_i U - m\gamma \frac{d\mathbf{r}_i}{dt} + \mathbf{W}_i(t), \quad (2)$$

where m is the counterion mass, U is the potential force having two contributions: the Coulomb interaction and the excluded volume interaction, and γ is the friction coefficient. Friction and stochastic force are linked by the dissipation-fluctuation theorem $\langle \mathbf{W}_i(t) \cdot \mathbf{W}_j(t') \rangle = 6m\gamma k_B T \delta_{ij} \delta(t - t')$. For the ground state simulations the fluctuation force is set to zero.

Excluded volume interactions are taken into account with a purely repulsive Lennard-Jones potential given by

$$U_{LJ}(r) = \begin{cases} 4\epsilon_{LJ} \left[\left(\frac{\sigma}{r-r_0} \right)^{12} - \left(\frac{\sigma}{r-r_0} \right)^6 \right] + \epsilon_{LJ}, & \text{for } r - r_0 < r_{cut}, \\ 0, & \text{for } r - r_0 \geq r_{cut}, \end{cases} \quad (3)$$

where $r_0 = 0$ for the counterion-counterion interaction, $r_0 = 7\sigma$ for the macroion-counterion interaction, r_{cut} ($= 2^{1/6}\sigma$) is the cutoff radius. This leads to an *effective* macroion radius a ($a = r_0 + \sigma = 8\sigma$) corresponding physically to the macroion-counterion distance of closest approach. Energy and length units in our simulations are defined as $\epsilon_{LJ} = k_B T_0$ (with $T_0 = 298$ K) and $\sigma = 3.57$ Å respectively. In the following we will set $k_B T_0 = 1$, so that all energies are measured in those units, suppressing thereby all factors of $k_B T_0$ in our equations.

The pair electrostatic interaction between any pair ij , where i and j denote either a macroion or a counterion, reads

$$U_{coul}(r) = l_B \frac{Z_i Z_j}{r}, \quad (4)$$

where Z_i represents the valence of the ions (counterion or macroion). Being essentially interested in the strong Coulomb coupling regime we choose the relative permittivity $\epsilon_r = 16$, corresponding to a Bjerrum length of 10σ , for the remaining of this paper. To avoid image charges complications, the permittivity ϵ_r is supposed to be identical within whole the cell (including the macroion) as well as outside the cell. Typical simulation parameters are gathered in Table I.

IV. ONE MACROION CASE

In this section, we focus on counterion distribution exclusively governed by *energy minimization*, i. e. $T = 0\text{K}$. The single spherical macroion is fixed to the center of the large outer spherical simulation cell (i. e. both spheres are concentric). In such a case correlations are maximal, and all the counterions lie on the surface of the spherical macroion. To avoid being trapped in metastable states, we systematically heated and cooled (10 cycles) the system and only kept the lowest energy state then obtained [24]. It turns out that for this type of repulsive potential (between counterions) no rough energy landscape appears and thus, the MD method is efficient to find the ground state. First, we checked that this method reproduces well the ground state energies and structures of the simple situations depicted in Fig. 1.

A. Counterion distribution

To characterize the counterion layer *structure*, we compute the counterion correlation function $g(r)$ on the surface of the sphere, defined as:

$$c^2 g(r) = \sum_{i \neq j} \delta(r - r_i) \delta(r - r_j), \quad (5)$$

where $c = N/4\pi a^2$ is the surface counterion concentration (N being the number of counterions), r corresponds to the arc length on the sphere. Note that at zero temperature all

equilibrium configurations are identical, thus only one is required to obtain $g(r)$. The pair distribution $g(r)$ is normalized as follows

$$c \int_0^{\pi a} 2\pi r g(r) dr = (N_c + n - 1), \quad (6)$$

where $N_c = Z_m/Z_c$ is the number of counterions in the neutral state and n is the number of overcharging counterions. Because of the *finite* size and the topology of the sphere, $g(r)$ has a cut-off at πa ($= 25.1 \sigma$) and a *zero* value there. More precisely one cannot state that the uncorrelated case corresponds to $g(r) = 1$ for the present finite system. Therefore at “large” distance the correlation function differs from the one obtained with an infinite planar object. Furthermore the absolute value of $g(r)$ cannot be directly compared to the one obtained with an infinite plane.

Correlation functions for the structural charge $Z_m = 180$ and for two states of charge, neutral ($n = 0$) and overcharged ($n = 8$), can be inspected in Fig. 2. One remarks that both structures are very similar and highly ordered. A snapshot of the ground state structure of the neutral state ($n = 0$) is depicted in Fig. 3. A visual inspection gives an almost perfect *triangular* crystalline structure (see Fig. 3). A closer look at Fig. 2 reveals that the $g(r)$ of the overcharged state, containing eight more counterions than the neutral one, shows its first peak at some shorter distance compared to the $g(r)$ of the neutral state, as is expected for denser systems.

It is also interesting to know how the counterion-layer structure looks like when the system is brought to *room temperature* T_0 . At non zero temperature, correlation functions are computed by averaging $\sum_{i \neq j} \delta(r - r_i)\delta(r - r_j)$ over 1000 independent equilibrium configurations which are statistically uncorrelated. Results are depicted in Fig. 4 for $Z_m = 180$ and $f_m = 8 \times 10^{-3}$. As expected the long-range counterion positional order is neatly weaker at room temperature than in the ground state case. Meanwhile, the structure remains very correlated and highly short-range ordered and therefore it is referred as a strongly correlated liquid (SCL) [25]. In terms of Coulomb coupling parameter [25,26] $\Gamma = \ell/a_{cc}$, where a_{cc} is the average distance between counterions, we have $\Gamma \approx 13$ for $Z_m = 180$.

B. Energy analysis

As demonstrated in Sec. II, the spatial correlations are fundamental to obtain overcharge. Indeed, if we apply the same procedure and smear Z counterions onto the surface of the colloid of radius a , we obtain for the energy

$$E = l_B \left[\frac{1}{2} \frac{Z^2}{a} - \frac{Z_m Z}{a} \right]. \quad (7)$$

The minimum is reached for $Z = Z_m$, hence no overcharging occurs.

To generalize results of Sec. II to higher central charges we have considered three macroionic charge Z_m of values 50, 90 and 180 corresponding to a surface charge density of one elementary charge per 180, 100 and 50 \AA^2 , respectively. For a given macroion, we always start by adding the exact number of counterions N_c to have an electro-neutral system. Once equilibrium of this system is reached, we add the first overcharging counterion and let the new non-neutral system relax, and we repeat this operation a given number of times. The electrostatic energy is computed by summing up the pairwise interactions of Eq. (4) over all pairs.

The electrostatic energy as a function of the number of overcharging counterions n is displayed Fig. 5. We note that the maximal (critical) acceptance of n (4, 6 and 8) increases with the macroionic charge Z_m (50, 90 and 180 respectively). Furthermore for fixed n , the gain in energy is always increasing with Z_m . Also, for a given macroionic charge, the gain in energy between two successive overcharged states is decreasing with n .

The results of Sec. IV A showed that in the ground state the counterions were highly ordered. Rouzina and Bloomfield [26] first stressed the special importance of these crystalline arrays for interactions of multivalent ions with DNA strands, and later Shklovskii ([12,25] and references therein) showed that the Wigner crystal (WC) theory can be applied to determine the interactions in strongly correlated systems. In two recent short contributions [19,20] we showed that the overcharging curves obtained by simulations of the ground state, like Fig. 5, can be simply explained by assuming that the energy ε per counterion on

the surface of a macroion depends linearly on the inverse distance between them, hence is proportional to \sqrt{N} for fixed macroion area, where N is the *total* number of counterions on the surface [19,20,27]. This can be justified by the WC theory. The idea is that the counterions form an ordered lattice on the surface of a homogeneously charged background of opposite charge. Each ion interacts in first approximation only with the oppositely charged background of its Wigner-Seitz (WS) cell [25], which can be approximated by a disk of radius h , which possesses the same area as the WS cell. Because we can assume the area of the WS cell to be evenly distributed among the N counterions on the sphere's surface $A = 4\pi a^2$ we find

$$\pi h^2 = \frac{A}{N} = c^{-1}. \quad (8)$$

The electrostatic interaction energy $\varepsilon^{(h)}$ of one counterion with the background of its WS cell can then be determined by

$$\epsilon^{(h)} = -l_B Z_c^2 \int_0^h 2\pi r c \frac{1}{r} dr = -2\sqrt{\pi} l_B Z_c^2 \sqrt{c}, \quad (9)$$

hence is proportional to \sqrt{c} , which proves our initial assumption. It is convenient to define $\ell = l_B Z_c^2$ and $\alpha^{(h)} = 2\sqrt{\pi} \approx 3.54$. For fixed macroion area we can then rewrite Eq. (9) as

$$\varepsilon^{(h)}(N) = -\frac{\alpha^{(h)} \ell}{\sqrt{A}} \sqrt{N}. \quad (10)$$

If one computes this value for an infinite plane, where the counterions form an exact triangular lattice, and takes into account all interactions, one obtains the same form as in Eq. (9), but the prefactor $\alpha^{(h)}$ gets replaced by the numerical value $\alpha^{WC} = 1.96$ [28]. Although the *value* is almost a factor of two smaller than the simple hole picture suggests, the *functional dependence* on the concentration is still the same.

Not knowing the precise value of α we can still use the simple scaling behavior with c to set up an equation to quantify the energy gain ΔE_1 by adding the first overcharging counterion to the colloid. The energy gained (relative to the neutral state) is a pure correlation term and should look like

$$\Delta E_1 = (N_c + 1)\varepsilon(N_c + 1) - N_c\varepsilon(N_c). \quad (11)$$

By using Eq. (10) this can be rewritten as

$$\Delta E_1 = -\frac{\alpha\ell}{\sqrt{A}} \left[(N_c + 1)^{3/2} - N_c^{3/2} \right]. \quad (12)$$

For the next overcharging counterion one has to take into account the Coulomb repulsion term ℓ/a , which can be summed up for the n^{th} overcharging counterion as $\frac{(n-1)n}{2}\frac{\ell}{a}$. This leads to the energy gain ΔE_n for n overcharging counterions which is given by

$$\Delta E_n = -\frac{\alpha\ell}{\sqrt{A}} \left[(N_c + n)^{3/2} - N_c^{3/2} \right] + \frac{\ell}{a} \frac{(n-1)n}{2}. \quad (13)$$

Equation (13) can be seen as an approximation of the exact general expression Eq. (1), where the topological term $f(\theta)$ is handled by assuming a perfect planar crystalline structure through Eqs. (11-13). Using Eq. (13), where we determined the unknown α from the simulation data for ΔE_1 via Eq. (12) we obtain a curve that matches the simulation data almost perfectly, compare Fig. 5. The second term in Equation (13) also shows why the overcharging curves of Fig. 5 are shaped parabolically upwards for larger values of n .

Using the measured value of α we can simply determine the maximally obtainable number n_{max} of overcharging counterions by finding the stationary point of Eq. (13) with respect to n :

$$n_{max} = \frac{1}{2} + \frac{9\alpha^2}{32\pi} + \frac{3\alpha}{4\sqrt{\pi}} \sqrt{N_c} \left[1 + \frac{1 + \frac{9\alpha^2}{32\pi}}{2N_c} \right]^{1/2}. \quad (14)$$

The value of n_{max} depends only on the number of counterions N_c and α . For large N_c Eq. (14) reduces to $n_{max} \approx \frac{3\alpha}{4\sqrt{\pi}} \sqrt{N_c}$ which was derived in Ref. [25] as the low temperature limit of a neutral system in the presence of salt. What we have shown is that the overcharging in this limit has a pure electrostatic origin, namely it originates from the topological favorable arrangement of the ions around a central charge. In the following we will investigate the behavior of α on the surface charge density and on the radius of the macroion.

We have performed simulations for various surface charge densities by keeping A fixed and changing $Z_m = 2N_c$ in the range 2 up to 180. Results can be found in Table II and in

Fig. 6. We observe that α increases for small values of N_c and reaches a limiting value of $\alpha = 1.75 \pm 0.05$ already with $N_c = 25$. This value is about 10% smaller than the one predicted by WC theory, and is presumably due to the finite curvature of the sphere. For large values of the radius a we expect α to reach the planar limit. To see the rate of convergence we varied¹ a at a fixed concentration c . The results can be found in Table III and Fig. 7. For our smallest value of $a = 6\sigma$ we find $\alpha = 1.53$, whereas for our largest value $a = 80$ we find $\alpha = 1.94$, which is almost $\alpha^{WC} = 1.96$. Again we stress that the numerical value of α enters only as a prefactor into the equations which govern the overcharging, it does not change the qualitative behavior.

One could wonder if the results presented above are still valid when the bare central charge of the colloid is replaced by small *discrete* ions lying on the macroion surface? In fact it has been shown that the energy of the overcharged state (Fig. 5) for *random* discrete colloidal charge distribution is more or less quantitatively affected [29,30] depending on the the valence of the counterions. More precisely it was shown that the overcharge still persists and has a similar (for monovalent counterions) or quasi-identical (for multivalent counterions) behavior to the one depicted in Fig. 5, and this, even if *ionic pairing* occurs between the counterions and the discrete colloidal charges [29,30], that is even when *no* counterion WC is formed.

C. Macroion-counterion interaction profile

In this part, we study the interaction potential profile at $T = 0K$ between a *neutral effective* macroion [bare macroion + neutralizing counterions] and one excess overcharging counterion at a distance r from the colloid center. The profile is obtained by displacing adiabatically the excess overcharging counterion from infinity towards the macroion. We investigated the case of $Z_m = 2, 4, 6, 8, 10, 32, 50, 90, 128, 180$, and 288. All curves can be

¹Note that this is the only part of the paper where $a \neq 8\sigma$.

nicely fitted with an exponential fit of the form

$$E_1(r) = \Delta E_1 e^{-\tau(r-a)}, \quad (15)$$

where ΔE_1 is the measured value for the first overcharging counterion, and τ is the only fit parameter (see Table II). Results for the two values $Z_m = 50$ and 180 are depicted in Fig. 8. If one plots all our results for τ versus $\sqrt{N_c}$ we observe a linear dependence for a wide range of values for N_c ,

$$\tau = m\sqrt{N_c}, \quad (16)$$

with $m\sigma \approx 0.1$, as can be inspected in Fig. 9.

This behavior can again be explained using a “WC hole” picture in the limiting situation where $x := r - a$ is small (i. e. the displaced counterion is close to the macroion surface). To this end we consider the classical electrostatic interaction $V_{disk}(x)$ between a uniformly charged disk (the WC hole - supposed planar) and a point ion (the displaced counterion) located on the axis of the disk at a distance x from its surface, which is given by

$$V_{disk}(x) = -2\pi\ell c(\sqrt{h^2 + x^2} - x). \quad (17)$$

Like in Eq. (9), $h = (\pi c)^{-1/2}$ is the hole radius. For small distance x , we expand Eq. (17)

$$V_{disk}(x) = \varepsilon^{(h)} \left[1 - \frac{1}{h}x + \frac{1}{2h^2}x^2 + \mathcal{O}\left(\frac{x^4}{h^4}\right) \right], \quad (18)$$

where the surface term $V_{disk}(x = 0) = \varepsilon^{(h)}$ is given by Eq. (9). By expanding the exponential in Eq. (15) to 2^{nd} order for small τx we obtain

$$E_1(x) = \Delta E_1 \left[1 - \tau x + \frac{\tau^2}{2}x^2 + \mathcal{O}(\tau^3 x^3) \right]. \quad (19)$$

A comparison between Eq. (19) and Eq. (18) shows that to this order we can identify

$$\tau = \frac{1}{h} = \sqrt{\pi c} = \frac{\sqrt{N_c}}{2a} \approx 0.06\sqrt{N_c}. \quad (20)$$

Comparing this to Eq. (16) we note that this simple illustration gives us already the correct scaling as well as the prefactor up to 30%. We neglected here the effect that the surface concentration changes when the ion is close to the macroion as well as the curvature of the macroion.

V. TWO MACROIONS CASE

In this section we consider two fixed charged spheres of bare charge Q_A and Q_B separated by a center-center separation R and surrounded by their neutralizing counterions. All these ions making up the system are immersed in a cubic box of length $L = 80\sigma$, and the two macroions are held fixed and disposed symmetrically along the axis passing by the two centers of opposite faces. This leads to a colloid volume fraction $f_m = 2 \cdot \frac{4}{3}\pi(a/L)^3 \approx 8.4 \times 10^{-3}$. For *finite* colloidal volume fraction f_m and temperature, we know from the study carried out above that in the strong Coulomb coupling regime all counterions are located in a spherical “monolayer” in contact with the macroion. Here, we investigate the mechanism of *strong long range* attraction stemming from *monopole* contributions: that is one colloid is overcharged and the other one undercharged.

A. Like charged colloids

1. *Observation of metastable ionized states*

In the present charge symmetrical situation we have $Q_A = Q_B = -Z_m e$. This system is brought at *room temperature* T_0 . Initially the counterions are randomly generated inside the box. Figure 10 shows two macroions of bare charge $Z_m = 180$ surrounded by their quasi-two-dimensional counterions layer. The striking peculiarity in this configuration is that it corresponds to an overcharged and an undercharged sphere. There is one counterion more on the left sphere and one less on the right sphere compared to the bare colloid charge. Such a configuration is referred as *ionized state*. In a total of 10 typical runs, we observe this phenomenon 5 times. We have also carefully checked against a situation with periodic boundary conditions, yielding identical results. However it is clear that such a state is “metastable” because it is not the lowest energy state. Indeed, in this symmetrical situation the ground state should also be symmetrical so that both colloid should be exactly charge-compensated. Such arguments remain valid even at non-zero temperature as long as the

system is strongly energy dominated, which is presently the case. Nevertheless the ionized states observed here seem to have a long life time since even after 10^8 MD time steps this state survives. In fact we could not observe within the actual computation power the recover of the stable neutral state. To understand this phenomenon we are going to estimate the energy barrier involved in such a process.

2. Energy barrier and metastability

To estimate the energy barrier, electrostatic energy profiles at *zero temperature* were computed, where we move one counterion from the overcharged macroion to the undercharged, restoring the neutral state [see drawing depicted in Fig. 11(a)]. We have checked that the path leading to the lowest barrier of such a process corresponds to the line joining the two macroions centers. The simulation data are sketched in Figs. 11(a-b) and were fitted using a similar technique to the single macroion-counterion interaction profile given by Eq. (15), which will be explicitly treated later. The resulting simulated energy barrier ΔE_{bar} is obtained by taking the difference between the highest energy value of the profile and the ionized state energy (start configuration). Values of ΔE_{bar} can be found in Table IV for the small macroion separation case $R/a = 2.4$. One clearly observes a barrier, which increases quasi linearly with the charge Z_m for the small colloids separation $R/a = 2.4$ [cf. Fig. 11(a) and Table IV]. The ground state corresponds as expected to the neutral state. Note that the ionized state and the neutral state are separated by only a small energy amount (less than 2.5), the difference being approximately of the order of the monopole contribution $E = l_B(4/8 - 4/11) \approx 1.36$. The physical origin of this barrier can be understood from the single macroion case where we showed that a counterion gains high correlational energy near the surface. This gain is roughly equal for both macroion surfaces and decreases rapidly with increasing distance from the surfaces, leading to the energy barrier with its maximum near the midpoint. For the single macroion case we showed that the correlational energy gain scales with $\sqrt{Z_m}$, whereas here we observe a linear behavior of the barrier height with

Z_m . We attribute this effect to additional ionic correlations since both macroions are close enough for their surface ions to interact strongly. For large separations (here $R/a = 4.25$) we find again that the barrier height increases with $\sqrt{Z_m}$, as expected [see Fig. 11(b) and Table V]. Furthermore the energy barrier height naturally increases with larger colloidal separation. The Z_m dependence of the barrier also shows that at room temperature such ionized states only can occur for large Z_m . In our case only for $Z_m = 180$, the ionized state was stable for all accessible computation times. Unfortunately, it is not possible to get a satisfactory accuracy of the energy jumps at non-zero temperatures. Nevertheless, since we are interested in the strong Coulomb coupling regime, which is energy dominated, the zero temperature analysis is sufficient to capture the essential physics.

Simulation results presented in Fig. 11 can be again theoretically well described using the previously exponential profiles obtained for the macroion-displaced counterion in Sec. IV C for a *single* colloid. For the two macroions case, the general expression for the electrostatic interaction $E_{bar}(r, R)$ of the present process can be approximated as

$$E_{bar}(r, R) = \Delta E_1^* \exp[-\tau(r - a)] + \Delta E_1^* \exp[-\tau(R - r - a)] - \frac{\ell}{R - r}, \quad (21)$$

where ΔE_1^* is the “effective” *correlational* energy gained by the first OC at one macroion surface assumed identical for both colloids. The last term in Eq. (21) corresponds to the additional monopole attractive contribution of the displaced counterion with the undercharged colloid. Fitting parameters (ΔE_1^* and τ) for $R/a = 2.4$ and $R/a = 4.25$ can be found in Tables IV and V respectively. Same values of τ were used here as those of the single macroion case (see Fig. 9 and Table II). However for the small colloidal separation ($R/a = 2.4$), due to the extra inter-colloidal surface counterions correlations, we used a slightly larger (absolute) value for ΔE_1^* compared to the one (ΔE_1) of an isolated colloid (compare Tables IV and V). This is compatible with the idea that between the two colloids (especially when both spheres come at contact), we have the formation of a “super-layer” which is more dense, thus leading to a smaller hole radius and a higher energy gain. An analysis of the counterions structure of the two macroions reveals that both WC counterion layers are

interlocked, that is the projection along the axis passing through the colloid centers gives a superlattice structure (see Fig. 12).

For large colloidal separation ($R/a = 4.25$), the WC structure on one of the colloids is unperturbed by the presence of the other, hence we can take $\Delta E_1^* = \Delta E_1$, and our simulation data can nicely be fitted by the parameters inferred from the single colloid system.

3. Effective forces

Results concerning the effective forces at *zero temperature* between the two macroions are now investigated which expression is given by

$$F_{eff}(R) = F_{mm}(R) + F_{LJ} + F_{mc}, \quad (22)$$

where $F_{mm}(R)$ is the direct Coulomb force between macroions, F_{LJ} is the excluded volume force between a given macroion and its surrounding counterions and F_{mc} is the Coulomb force between a given macroion and all the counterions. Because of symmetry, we focus on one macroion. To understand the extra-attraction effect of these ionized-like states, we consider three cases: (i) $F_{ion} = F_{eff}$ in the ionized state with a charge asymmetry of ± 1 counterion (ii) $F_{neut} = F_{eff}$ in the neutral case (iii) $F_{mono} = F_{eff}$ simply from the effective monopole contribution. Our results are displayed in Fig. 13 for $Z_m = 180$, where the ionized state was also observed at room temperature. The non-compensated case leads to a very important extra attraction. This becomes drastic for the charge asymmetry of ± 2 counterions at short separation $R/a = 2.4$ leading to a reduced effective attractive force $F_{LB} = -10.7$, a situation which was also observed in our simulation at room temperature. In contrast to previous studies [15,16], these attractions are long range. For a sufficiently large macroion separation (from $3.5a$), corresponding here roughly to a macroion surface-surface separation of one colloid diameter, the effective force approaches in good approximation the monopole contribution (see Fig. 22).

B. Asymmetrically charged colloids

In this section we investigate the case where the two colloids have different charge densities. We will keep the colloidal radii a fixed, but vary the bare colloidal charges. The charge on sphere A is *fixed* at $Z_A = 180$, and sphere B carries *variable* charges with Z_B (where $Z_B < Z_A$) ranging from 30 up to 150. Global electroneutrality is ensured by adding $N_A + N_B$ divalent counterions, with $N_A = Z_A/Z_c$, and $N_B = Z_B/Z_c$. In this way we vary the bare counterion concentrations $c_i = \sqrt{N_i/4\pi a^2}$, where i stands for A or B .

1. Ground state analysis

We start out again with studying the ground state of such a system. The electrostatic energy of the system is investigated for different uncompensated bare charge cases (ionized states) by simply summing up Eq. (4) over all Coulomb pairs. We define the *degree of ionization (DI)* as the number of counterions overcharging colloid A (or, equivalently, undercharging colloid B). The system is prepared in various DI and we measure the respective energies. These states are separated by kinetic energy barriers, as was demonstrated above. We consider three typical macroionic charges Z_B (30, 90 and 150) and separations R/a (2.4, 3.0 and 4.25). The main results of the present section are given in Fig. 14. For the largest separation $R/a = 4.25$ and largest charge $Z_B = 150$ [see Fig. 14(a)], one notices that the ground state corresponds to the classical compensated bare charge situation [referred as the *neutral state (DI=0)*]. Moreover the energy increases stronger than linear with the degree of ionization. If one diminishes the bare charge Z_B to 90 and 30, the *ground state* is actually the ionized state for a DI of 1 and 3, respectively. The ionized ground state is about 8 and 36, respectively, lower in energy compared to the neutral state. This shows that even for a relative large colloid separation, stable ionized states should exist for sufficient low temperatures and that their stability is a function of their charge asymmetry.

For a shorter separation $R/a = 3.0$, ionized ground states are found [see Fig. 14(b)] for

the same charges Z_B as previously. Nevertheless, in the ground state the DI is now increased and it corresponds to 2 and 4 for $Z_B = 90$ and 30 respectively. The gain in energy is also significantly enhanced. For the shortest separation under consideration $R/a = 2.4$ [see Fig. 14(c)], the ground state corresponds for *all* investigated values of Z_B to the ionized state, even for $Z_B = 150$. We conclude that decreasing the macroion separation R enhances the DI and the stability of the ionized state.

To understand this ionization phenomenon, it is sufficient to refer to an *isolated* macroion surrounded by its neutralizing counterions. We have investigated the energies involved in the ionization (taking out counterions). The complementary process of overcharging (adding counterions) has already been investigated (see Fig. 5). A derivation of the formula describing the ionization energy ΔE^{ion} proceeds completely analogously to the one carried out for the overcharging Eq. (13) and gives for the n^{th} degree of ionization

$$\Delta E_n^{ion} = \frac{3n\alpha^B\ell}{2\sqrt{A}}\sqrt{N_B}\left[1 - \frac{n}{4N_B} + \mathcal{O}\left(\frac{1}{N_B^2}\right)\right] + \ell\frac{(n+1)n}{2a}. \quad (23)$$

In Fig. 15 we compare the predictions of Eqs. (13, 23) to our simulation data, which shows excellent agreement. Our numerical data for ΔE_1^{ion} for $N_B = 15, 45$, and 75 , the value of ΔE_1^{OC} for $N_A = 90$ (overcharging process), as well as the corresponding values for α , which have been used for Fig. 15 can be found in Table II.

With the help of Eqs. (13, 23), one can try to predict the curves of Fig. 14 for finite center-center separation R . Using for colloid A and B the measured values α^A and α^B , we obtain for the electrostatic energy difference at finite center-center separation R

$$\Delta E_n(R) = \Delta E_n^{ion} + \Delta E_n^{OC} = \frac{3n\alpha^B\ell}{2\sqrt{A}}\sqrt{N_B}\left[1 - \frac{n}{4N_B}\right] - \frac{3n\alpha^A\ell}{2\sqrt{A}}\sqrt{N_A}\left[1 + \frac{n}{4N_A}\right] + \ell\frac{n^2}{a}\left(1 - \frac{a}{R}\right). \quad (24)$$

The quality of the theoretical curves can be inspected in Fig. 14. The prediction is very good for large separations, but the discrepancies become larger for smaller separations, and one observes that the actual simulated energies are lower. The physical interpretation of Eq. (24) is straightforward. The left two terms represent the difference in correlation energy, and

last term on the right the monopole penalty due to the ionization and overcharging process. This means that the correlational energy gained by overcharging the highly charged colloid *A* must overcome the loss of correlation energy as well as the monopole contribution (*two* penalties) involved in the ionization of colloid *B*. With the help of Eq. (24) we can establish a simple criterion (more specifically a sufficient condition), valid for large macroionic separations, for the charge asymmetry $\sqrt{N_A} - \sqrt{N_B}$ to produce an ionized ground state of two unlike charged colloids with the same size:

$$\left(\sqrt{N_A} - \sqrt{N_B} \right) > \frac{4\sqrt{\pi}}{3\alpha^A}. \quad (25)$$

Referring to Fig. (15) this criterion is met when the overcharge curve (changed sign) is higher than the ionization curve.

If one uses the parameters of the present study one finds the requirement $N_B < 66$ to get a stable ionized state. This is consistent with our findings where we show in Fig. 14 that for $N_B = 75$, and $R/a = 4.25$, no ionized ground state exists whereas for $N_B = 60$ we observed one even for infinite separation (not reported here). The criterion Eq. (25) is merely a sufficient condition, since we showed in Fig. 14 that when the colloids are close enough this ionized state can appear even for smaller macroion charge asymmetry due to enhanced inter-colloidal correlations. At this stage, we would like to stress again, that the appearance of a stable ionized ground state is due merely to correlation. An analogous consideration with smeared out counterion distributions along the lines of Eq. (7) will again always lead to two colloids exactly neutralized by their counterions [31]. Our energetical arguments are quite different from the situation encountered at finite temperatures, because in this case even a Poisson-Boltzmann description would lead to an asymmetric counterion distribution. However, in the latter case this happens due to pure entropic reasons, namely in the limit of high temperatures, the counterions want to be evenly distributed in space, leading to an effective charge asymmetry.

At this stage, on looking at the results presented above, it appears natural and straightforward to establish an analogy with the concept of ionic bonding. It is well known in

chemistry that the electro-negativity concept provides a simple yet powerful way to predict the nature of the chemical bonding [32]. If one refers to the original definition of the electro-negativity given by Pauling [32]: “the power of an atom in a molecule to attract electrons to itself”, the role of the bare charge asymmetry becomes obvious. Indeed, it has an equivalent role at the mesoscopic scale as the electron affinity at the microscopic scale. Another interesting analogy is the influence of the colloidal separation on the stability of the ionized state. Like in diatomic molecules, the ionized state will be (very) stable only for sufficiently short colloid separations. Nevertheless, one should not push this analogy too far. One point where it breaks down concerns the existence of an ionized ground state in colloidal system for *large* colloid separation, providing that the difference in the counterion concentration on the surface is large enough. In an atomistic system this is impossible since even for the most favorable thermodynamical case, namely CsCl, there is a cost in energy to transfer an electron from a cesium atom to a chlorine atom. Indeed, the smallest existing ionization energy (for Cs, 376 kJ mol⁻¹) is greater in magnitude than the largest existing electron affinity (for Cs, 349 kJ mol⁻¹). In other terms, for atoms separated by large distances in the gas phase, electron transfer to form ions is always energetically unfavorable.

2. Finite temperature analysis

As a last result, aimed at experimental verification, we show that an ionized state can also exist *spontaneously* at room temperature T_0 . Figure 16 shows the time evolution of the electrostatic energy of a system $Z_A = 180$ with $Z_B = 30$, $R/a = 2.4$ and $f_m = 7 \cdot 10^{-3}$, where the starting configuration is the neutral state ($DI = 0$). One clearly observes two jumps in energy, $\Delta E_1 = -19.5$ and $\Delta E_2 = -17.4$, which corresponds each to a counterion transfer from colloid B to colloid A . These values are consistent with the ones obtained for the ground state, which are -20.1 and -16.3 respectively. Note that this ionized state ($DI = 2$) is more stable than the neutral but is expected to be metastable, since it was shown previously that the most stable ground state corresponds to $DI = 5$. The other stable

ionized states for higher DI are not accessible with reasonable computer time because of the high energy barrier made up of the correlational term and the monopole term which increases with DI . In Fig. 17 we display a typical snapshot of the ionized state ($DI = 2$) of this system at room temperature.

Obviously, these results are not expected by a DLVO theory even in the asymmetric case (see e. g. [33]). Previous simulations of asymmetric (charge and size) spherical macroions [34] were also far away to predict such a phenomenon since the Coulomb coupling was weak (water, monovalent counterions).

VI. CONCLUDING REMARKS

In summary, we have shown that the ground state of a charged sphere in the presence of excess counterions is *always* overcharged. A sufficiently charged colloid can in principle be highly overcharged due to counterion mediated correlation effects, and this phenomenon is quantitatively well described by a simple version of Wigner crystal theory. In the strong Coulomb coupling regime, the energy gain of a single excess ion close to a counterion layer can be of the order of many tens of $k_B T_0$. Furthermore we demonstrated that the electrostatic interaction between a counterion and a macroion effectively neutralized by its counterions decays exponentially on a length scale which is equal to the Wigner crystal hole radius.

We further found that for two *like-charged* macroions (symmetric case), an initially randomly placed counterion cloud of their neutralizing divalent counterions may not be equally distributed after relaxation, leading to two macroions of opposite net charges. This is due to the short range WC attraction which leads to this energetically favorable overcharged state. The resulting configuration is metastable, however separated by an energy barrier of several $k_B T_0$ when the bare charge is sufficiently large, and can thus survive for long times. Such configuration possess a natural strong long range attraction.

In return, if the symmetry in the counterion concentration on the colloidal surface is sufficiently broken, the ionized state can be *stable*. The ground state of such a system is

mainly governed by two important parameters, namely the asymmetry in the counterion concentration determined by $\sqrt{c_A} - \sqrt{c_B}$, and the colloid separation R . If the counterion concentration difference is high enough, the ground state corresponds to an ionized state, whatever the macroions separation R is. However, the degree of ionization depends on R . Besides, for large R , we have established a criterion, allowing to predict when a stable ionized configuration can be expected. The counterion concentration difference plays an analogous role to the electron affinity between two atoms forming a molecule with ionic bonding. We demonstrated that the results presented here for the ground state can lead to a stable ionic state even at room temperature providing that the Coulomb coupling and/or the counterion concentration asymmetry is sufficiently large. This is also a possible mechanism which could lead to strong long range attractions, even in bulk. Future work will treat the case where salt ions are present.

ACKNOWLEDGMENTS

This work is supported by *Laboratoires Européens Associés* (LEA) and a computer time grant hkf06 from NIC Jülich. We acknowledge helpful discussions with B. Jönsson, R. Kjellander, H. Schiessel, and B. Shklovskii.

REFERENCES

- [1] D. H. Everett, *Basic Principles of Colloidal Science* (Royal Society Of Chemistry, London, 1988).
- [2] M. Kepler and S. Fraden, Phys. Rev. Lett. **73**, 356 (1994).
- [3] J. C. Crocker and D. G. Grier, Phys. Rev. Lett. **77**, 352 (1994).
- [4] D. G. Grier and J. C. Crocker, Nature **385**, 230 (1997).
- [5] B. V. Derjaguin and L. D. Landau, Acta Physicochim. (USSR) **14**, 633 (1941).
- [6] E. J. Verwey and J. T. G. Overbeek, *Theory of the stability of Lyophobic Colloids* (Elsevier, Amsterdam, 1948).
- [7] T. M. Squires and M. P. Brenner, Phys. Rev. Lett. **85**, 4976 (2000).
- [8] N. Ise *et al.*, J. Chem. Phys. **78**, 536 (1983).
- [9] K. Ito, H. Yoshida, and N. Ise, Science **263**, 66 (1994).
- [10] B. V. R. Tata, E. Yamahara, P. V. Rajamani, and N. Ise, Phys. Rev. Lett. **78**, 2660 (1997).
- [11] R. van Roij and J.-P. Hansen, Phys. Rev. Lett. **79**, 3082 (1997).
- [12] B. Shklovskii, Phys. Rev. Lett. **82**, 3268 (1999).
- [13] R. R. Netz and H. Orland, Europhys. Lett. **45**, 726 (1999).
- [14] M. Tokuyama, Phys. Rev. E **59**, R2550 (1999).
- [15] N. Grønbech-Jensen, K. M. Beardmore, and P. Pincus, Physica **261A**, 74 (1998).
- [16] E. Allahyarov, I. D'Amico, and H. Löwen, Phys. Rev. Lett. **81**, 1334 (1998).
- [17] J. Z. Wu, D. Bratko, H. W. Blanch, and J. M. Prausnitz, J. Chem. Phys. **111**, 7084 (1999).

- [18] P. Linse and V. Lobaskin, Phys. Rev. Lett. **83**, 4208 (1999).
- [19] R. Messina, C. Holm, and K. Kremer, Phys. Rev. Lett. **85**, 872 (2000).
- [20] R. Messina, C. Holm, and K. Kremer, Europhys. Lett. **51**, 461 (2000).
- [21] A theory that predicts molecular geometries using the notion that valence electron pairs occupy sites around a central atom in such a way as to minimize electron-pair repulsion. See for example D. W. Oxtoby, H. P. Gillis and N. H. Nachtrieb, *Principles of Modern Chemistry* (Saunders College Publishing, 1999), Chap. 3, p. 80.
- [22] R. J. Gillespie, J. Chem. Educ. **40**, 295 (1963).
- [23] R. J. Gillespie, Struct. Chem. **9**, 73 (1998).
- [24] Since we are using (MD) simulations, to avoid barrier energy problem the counterions were generated in the vicinity of the colloidal surface.
- [25] B. Shklovskii, Phys. Rev. E **60**, 5802 (1999).
- [26] I. Rouzina and V. A. Bloomfield, J. Chem. Phys. **100**, 9977 (1996).
- [27] This is certainly justified if the counterion-counterion distance is smaller than the curvature radius of the macroion.
- [28] L. Bonsall and A. A. Maradudin, Phys. Rev. B **15**, 1959 (1977).
- [29] R. Messina, C. Holm, and K. Kremer, to be published, cond-mat/0006502.
- [30] R. Messina, C. Holm, and K. Kremer, in preparation.
- [31] H. Schiessel, private communication.
- [32] L. Pauling, *The nature of the chemical bond* (Cornell, Univ. Press, New York, 1939).
- [33] B. D'Aguanno and R. Klein, Phys. Rev. A **46**, 7652 (1992).
- [34] E. Allahyarov, H. Löwen, and S. Trigger, Phys. Rev. E **60**, 3199 (1999).

TABLES

TABLE I. Simulation parameters with some fixed values.

parameters	
$\sigma = 3.57 \text{ \AA}$	Lennard Jones length units
$T_0 = 298K$	room temperature
$\epsilon_{LJ} = k_B T_0$	Lennard Jones energy units
Z_m	macroion valence
$Z_c = 2$	counterion valence
$l_B = 10\sigma$	Bjerrum length
f_m	macroion volume fraction
$a = 8\sigma$	macroion-counterion distance of closest approach

TABLE II. Measured values for an *isolated* macroion, with fixed radius a , of the energy gain for the first overcharging counterion ΔE_1^{OC} for various macroion bare charge $Z_m = 2N_c$. The value of α can be compared to the prediction of WC theory for an infinite plane, which gives 1.96, compare text. We also record the values of the fitting parameter τ of Eq. (15) for selected N_c corresponding to those of Fig. (9). The symbol “(i)“ stands for the ionization process discussed in Sec. V B 1.

Z_m	N_c	$\Delta E_1/k_B T_0$	α	τ
2	1	-2.5	0.97	0.12
4	2	-3.8	1.15	0.18
6	3	-5.3	1.34	0.19
8	4	-6.1	1.35	0.24
10	5	-7.5	1.50	0.24
20	10	-10.7	1.56	-
30 ⁽ⁱ⁾	15	+17.9	1.60	-
32	16	-	-	0.41
50	25	-18.0	1.68	0.51
90	45	-24.4	1.71	0.68
90 ⁽ⁱ⁾	45	+29.2	1.72	-
128	64	-	-	0.79
150 ⁽ⁱ⁾	75	+37.4	1.76	-
180	90	-35.3	1.75	0.93
288	144	-	-	1.19
360	180	-50.0	1.76	-

TABLE III. Measured values of the energy gain ΔE_1^{OC} and fixed counterion concentration c , varying this time the macroion radius a and the number of counterions N_c .

a	N_c	$\Delta E_1/k_B T_0$	α
6	9	-13.3	1.53
8	16	-14.4	1.68
10	25	-14.5	1.69
12	36	-14.7	1.73
14	49	-15.1	1.78
16	64	-15.1	1.78
20	100	-15.3	1.81
40	400	-15.9	1.87
80	1600	-16.4	1.94

TABLE IV. Measured value of the energy barrier and fit parameters of the electrostatic interaction process involved in Fig. 11(a) for $R/a = 2.4$ and for different macroion bare charges.

Z_m	$\Delta E_{bar}/k_B T_0$	$\Delta E_1^*/k_B T_0$	$\tau\sigma$
50	4.9	-20.4	0.51
90	9.6	-27.5	0.68
180	20.4	-39.4	0.92

TABLE V. Measured value of the energy barrier and fit parameters of the electrostatic interaction process involved in Fig. 11(b) for $R/a = 4.25$ and for different macroion bare charges.

Z_m	$\Delta E_{bar}/k_B T_0$	$\Delta E_1^*/k_B T_0$	$\tau\sigma$
50	16.8	-18.4	0.51
90	23.3	-24.4	0.68
180	33.8	-35.3	0.92

FIGURES

FIG. 1. Ground state configurations for two, three, four and five counterions. The corresponding geometrical figures show the typical angles. The electrostatic energy (in units of $k_B T_0 l_B/a$) is given for a central charge of $+2e$.

FIG. 2. Ground state surface counterion correlation functions for $Z_m = 180$ and two states of charge [neutral ($n = 0$) and overcharged ($n = 8$)].

FIG. 3. Snapshot of the ground state structure of the neutral state ($n = 0$) with a macroion charge $Z_m = 180$ [see Fig. 2 for the corresponding $g(r)$].

FIG. 4. Surface counterion correlation functions at *room temperature* T_0 for two states of charge [neutral ($n=0$) and overcharged ($n=8$)] with $Z_m = 180$ and $f_m = 6.6 \times 10^{-3}$.

FIG. 5. Electrostatic energy (in units of $k_B T_0$) for *ground state* configurations of a single charged macroion of as a function of the number of *overcharging* counterions n for three different bare charges Z_m . The neutral case was chosen as the potential energy origin, and the curves were produced using the theory of Eq. (13), compare text.

FIG. 6. Wigner crystal parameter α as a function of the number of counterions N_c for fixed colloid radius a .

FIG. 7. Wigner crystal parameter α as a function of the colloid radius a for a fixed surface counterion concentration c .

FIG. 8. Electrostatic interaction energy (in units of $k_B T_0$) of a divalent counterion with a neutral effective colloid [bare particle + surrounded counterions] as function of distance r/a from the center of a macroion for two different macroion bare charges Z_m . The energy is set to zero at distance infinity. Solid lines correspond to exponential fits [see Eq. (15)].

FIG. 9. Exponential fit parameter τ as a function of the square root of the number of counterions $\sqrt{N_c}$. The dashed line corresponds to a linear fit in $\sqrt{N_c}$.

FIG. 10. Snapshot of a “pseudo-equilibrium” configuration at room temperature T_0 where the counterion-layers do not exactly compensate the macroions charge. Here the deficiency charge is ± 1 counterion (or $\pm 2e$ as indicated above the macroions) and $R/a = 3.6$.

FIG. 11. Total electrostatic energy (in units of $k_B T_0$) of the system, for *zero temperature* configurations, of two macroions at a center-center separation of (a) $R/a = 2.4$ (b) $R/a = 4.25$ as a function of one displaced counterion distance from the left macroion for three typical values Z_m . The exact neutral state was chosen as the potential energy origin. The schematic drawing indicates the path (dotted line) of the moved counterion. The ending arrows of the arc indicate the start position (left sphere) and final position (right sphere) of the moved counterion. Dashed lines correspond to the fit using Eq. (21) of which parameters can be found in Tables IV and V.

FIG. 12. Projection of the counterion positions, located on both inner (face to face) hemispheres, along the symmetrical axis passing through the macroion centers. Open (filled) circles are counterions belonging to macroion A (B). One clearly sees the interlocking of the two ordered structures yielding locally to a superlattice.

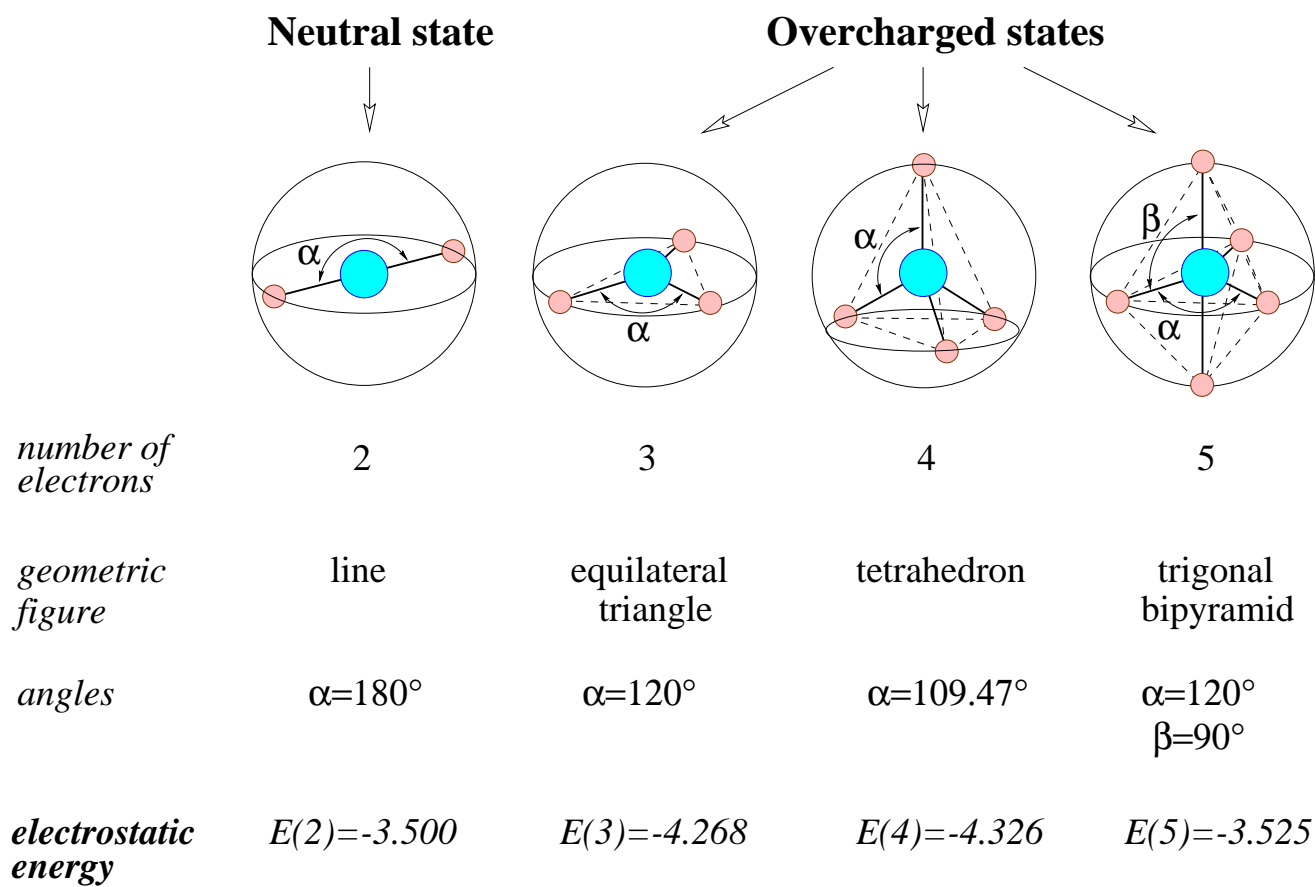
FIG. 13. Reduced effective force between the two spherical macroions at *zero temperature* for $Z_m = 180$ as a function of distance from the center. The different forces are explained in the text. The lines are a guide to the eye.

FIG. 14. Total electrostatic energy as a function of the degree of ionization for zero temperature configurations of two colloids (*A* and *B*), for three typical charges Z_B (30, 90 and 150) for macroion *B* and for three given distance separations: (a) $R/a = 4.25$, (b) $R/a = 3.0$ and (c) $R/a = 2.4$. Dashed lines were obtained using Eq. 24.

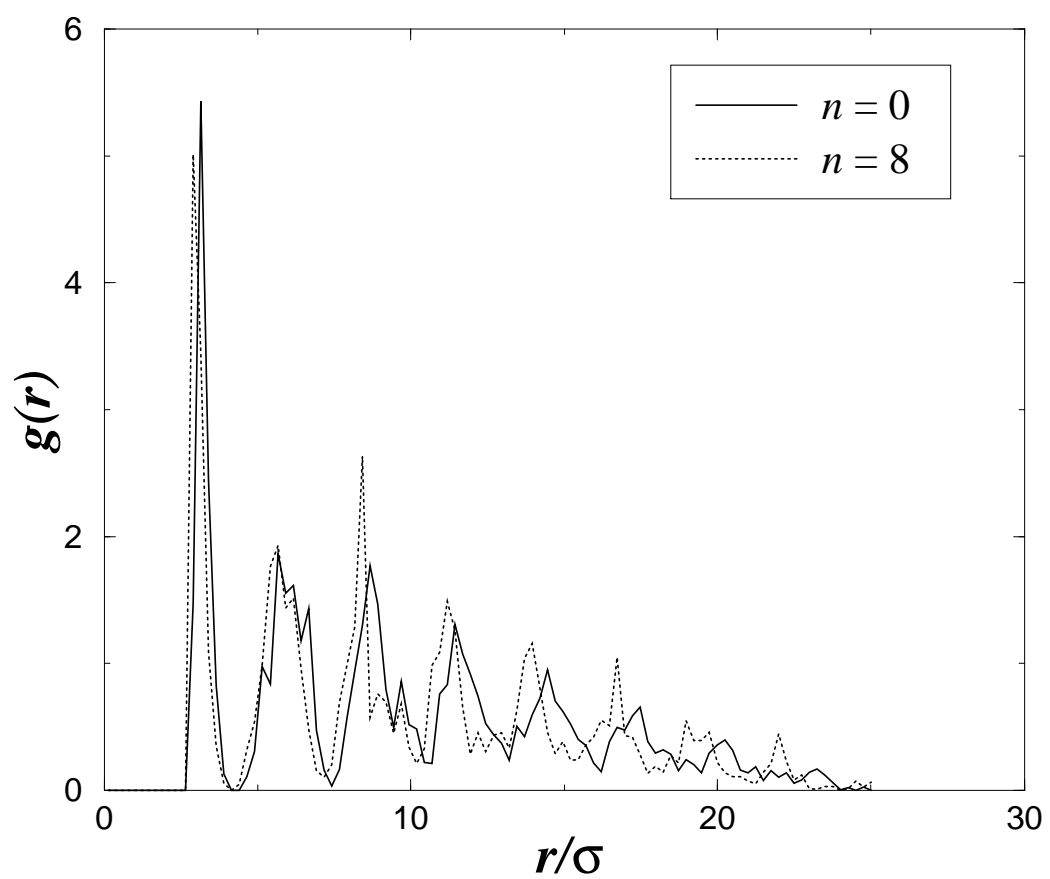
FIG. 15. Total electrostatic energy as a function of the degree of ionization for zero temperature configurations of an *isolated* colloid. The three upper curves correspond to the ionization energy for the three typical charges Z_B (30, 90 and 150). The lower curve corresponds to the energy gained (changed sign for commodity) by overcharging ($Z_A = 180$). Dashed lines were obtained using Eqs. (13, 23) with the measured values for α from Table II.

FIG. 16. Relaxation, at room temperature $T_0 = 298K$, of an initial unstable neutral state towards ionized state. Plotted is the total electrostatic energy versus time (LJ units), for $Z_B = 30$ and $R/a = 2.4$. Dashed lines represent the mean energy for each DI state. Each jump in energy corresponds to a counterion transfer from the macroion B to macroion A leading to an ionized state ($DI = 2$) which is lower in energy than the neutral one. The two energy jumps $\Delta E_1/k_B T_0 = -19.5$ and $\Delta E_2/k_B T_0 = -17.4$ are in very good agreement with those of Fig. 14(c) (-20.1 and -16.3).

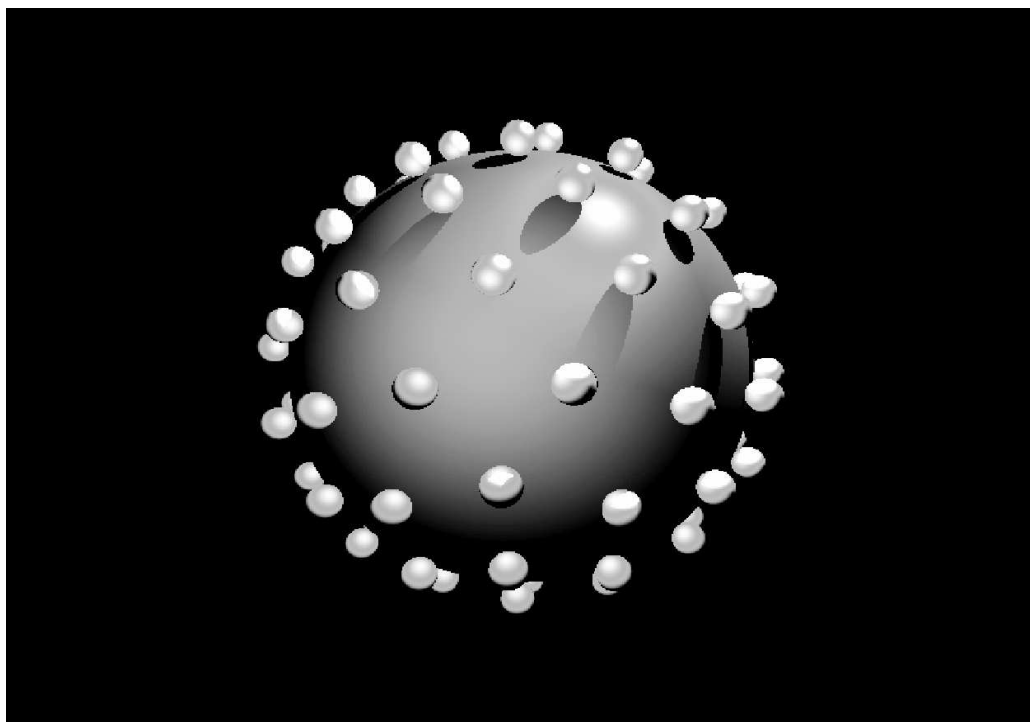
FIG. 17. Snapshot of the ionized state ($DI = 2$) obtained in the relaxation process depicted in Fig. 16, with the net charges $+4e$ and $-4e$ as indicated.



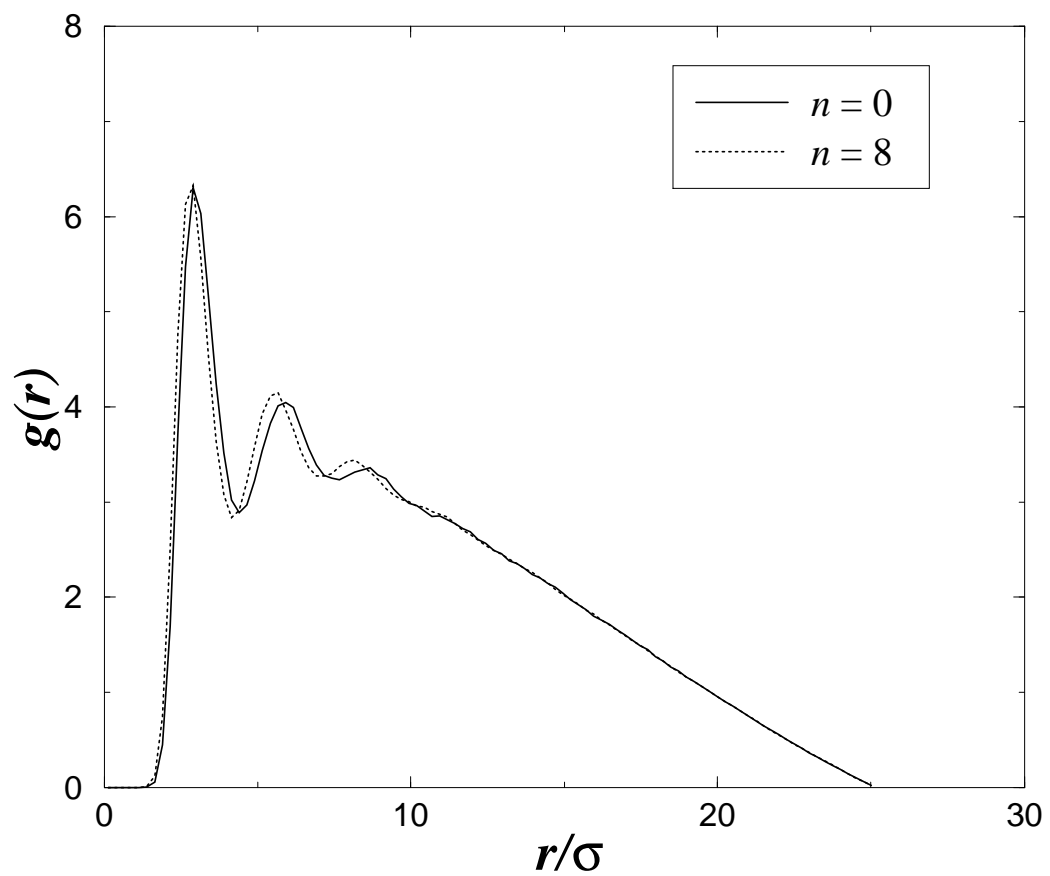
Messina et al.
Physical Review E
Figure 2



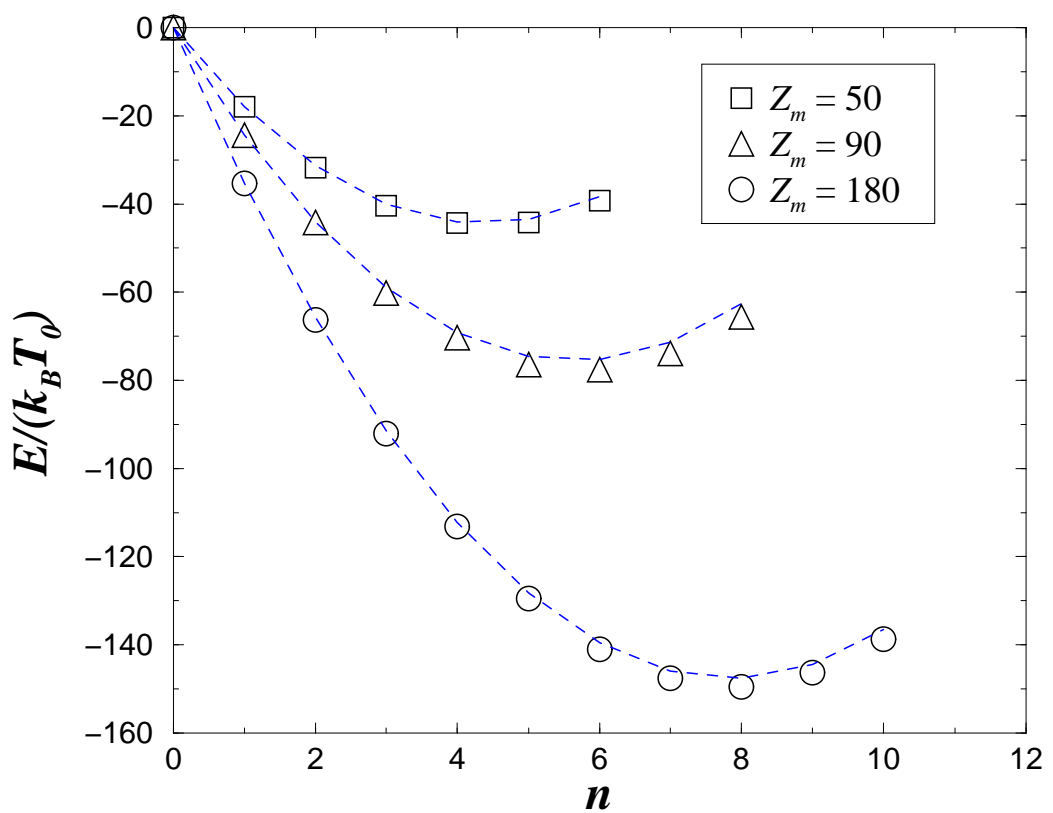
Messina et al.
Physical Review E
Figure 3



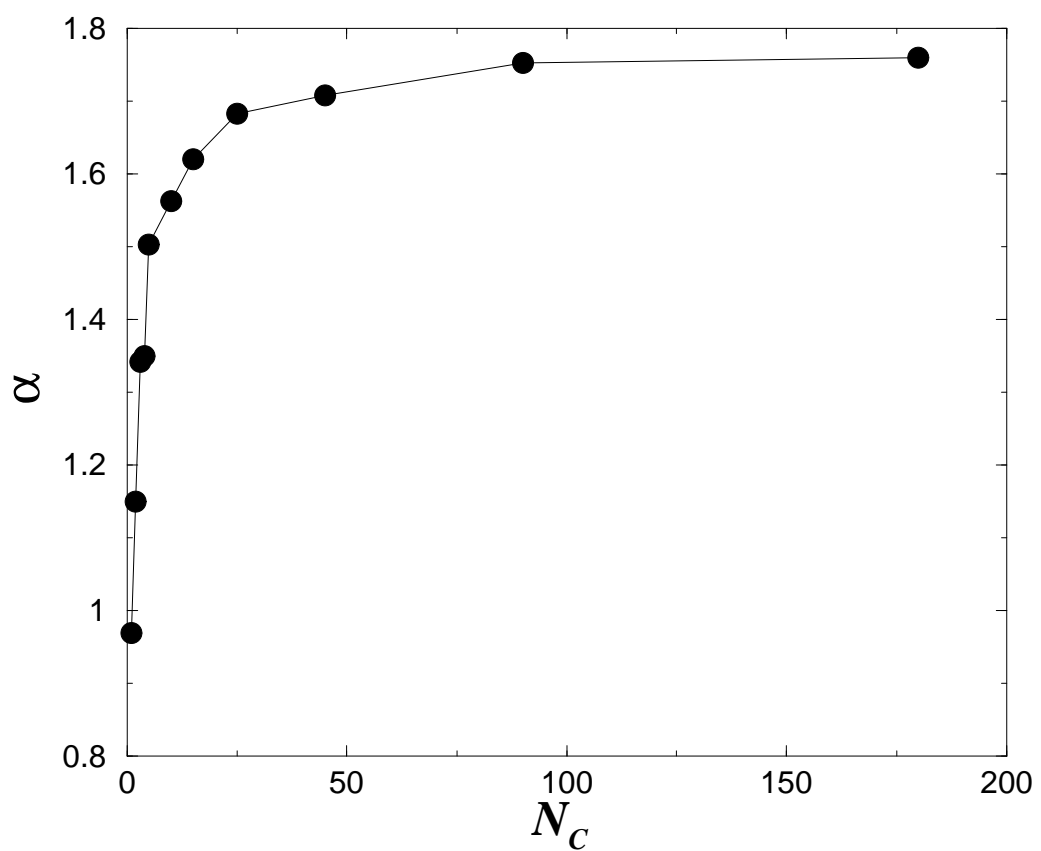
Messina et al.
Physical Review E
Figure 4



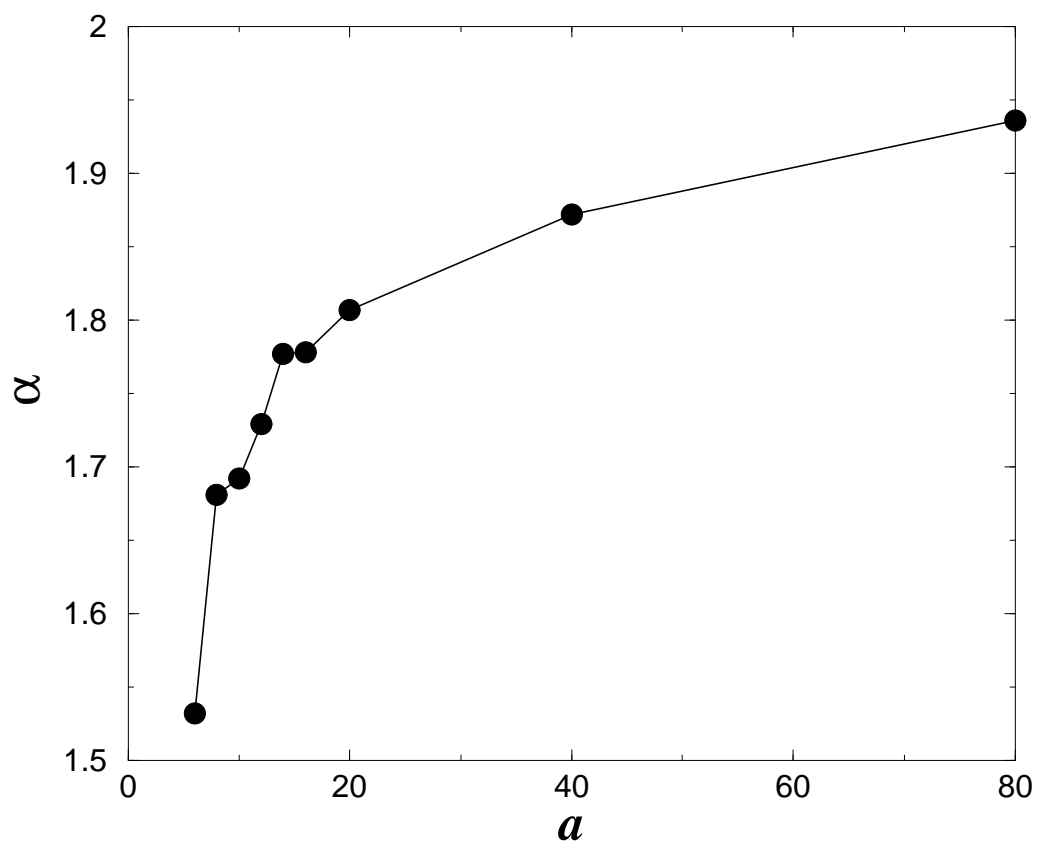
Messina et al.
Physical Review E
Figure 5



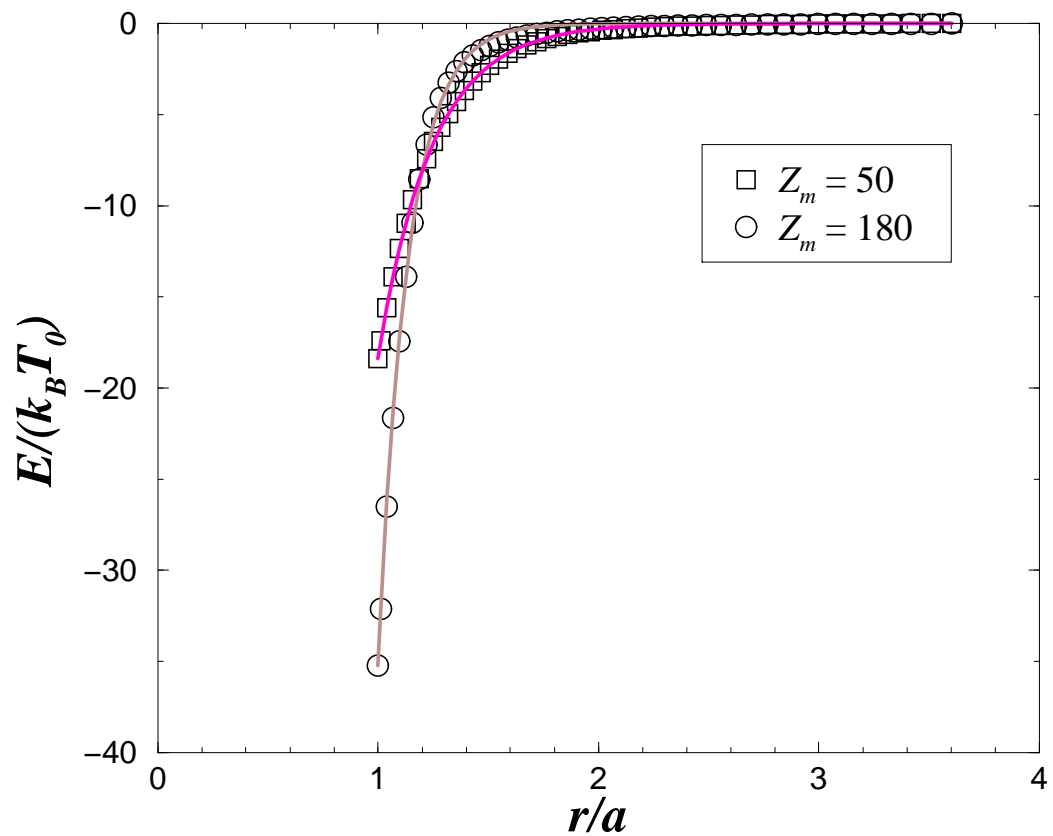
Messina et al.
Physical Review E
Figure 6



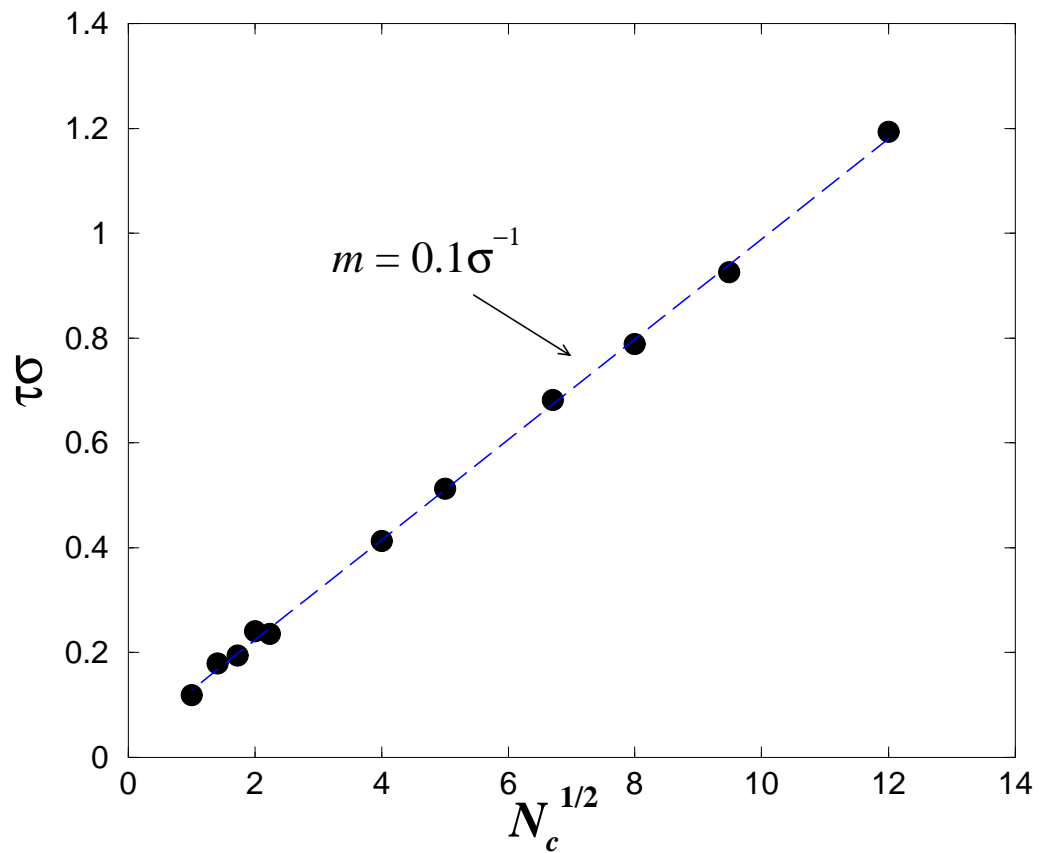
Messina et al.
Physical Review E
Figure 7



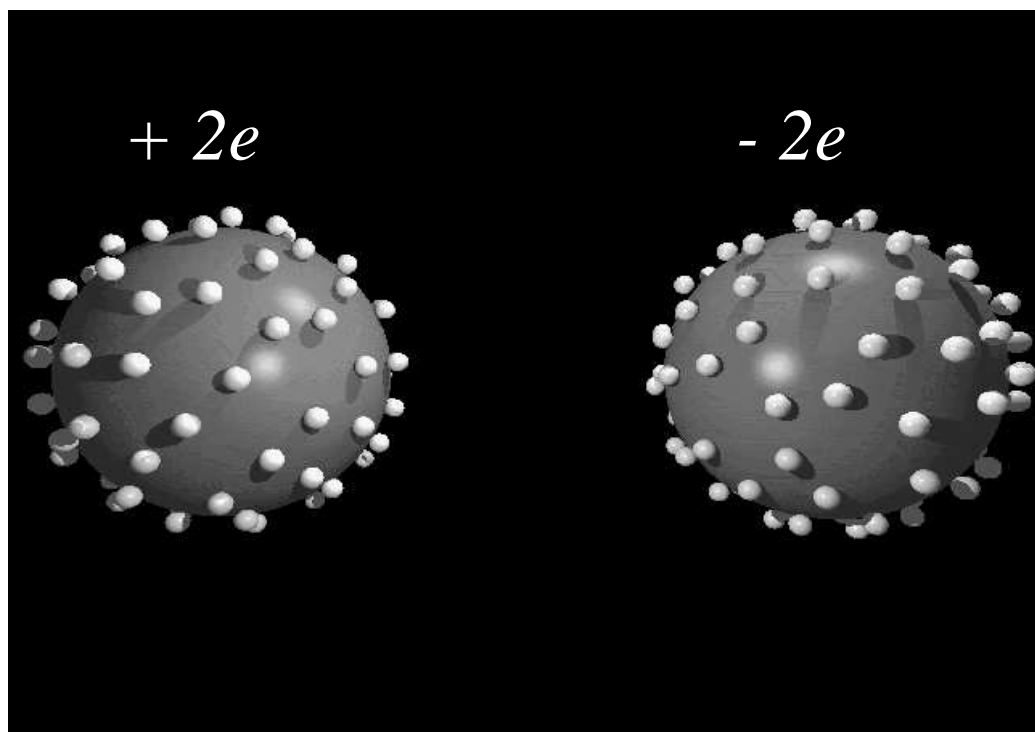
Messina et al.
Physical Review E
Figure 8



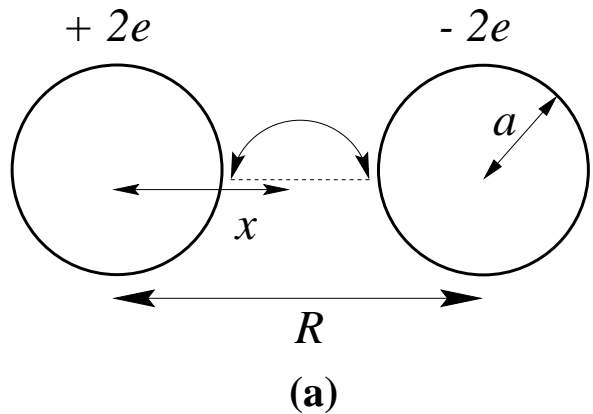
Messina et al.
Physical Review E
Figure 9



Messina et al.
Physical Review E
Figure 10

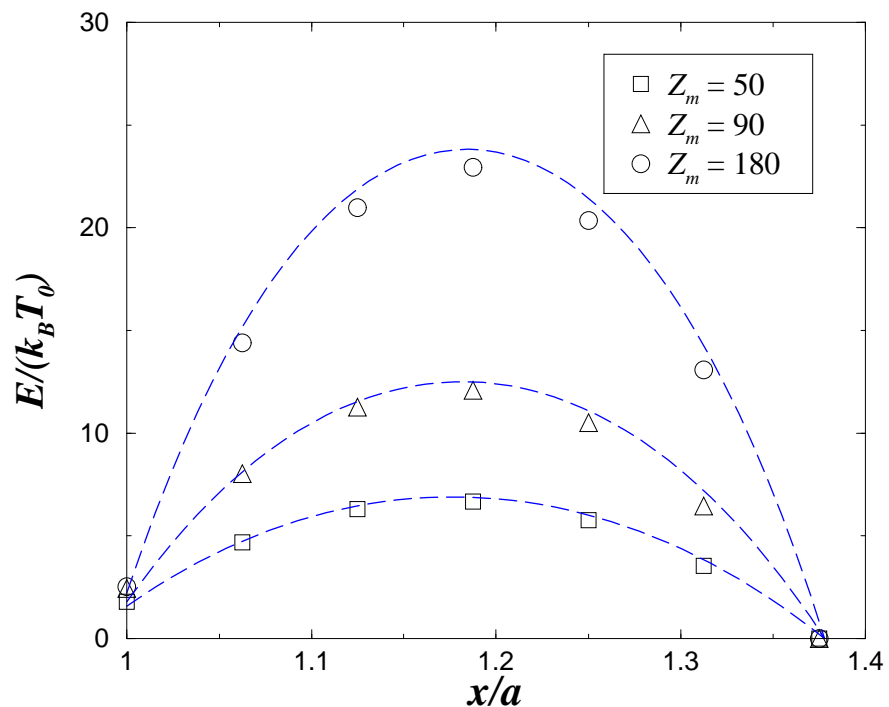


Messina et al.
Physical Review E
Figure 11 (a)

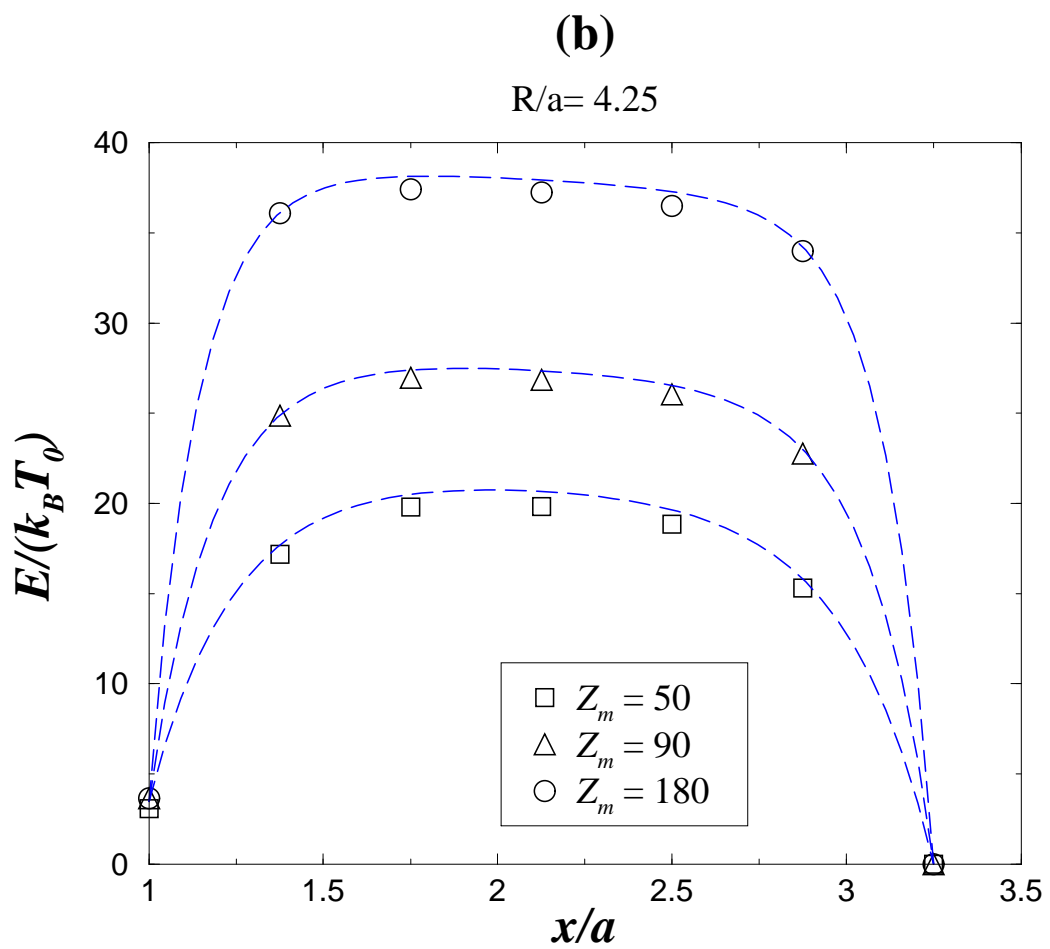


(a)

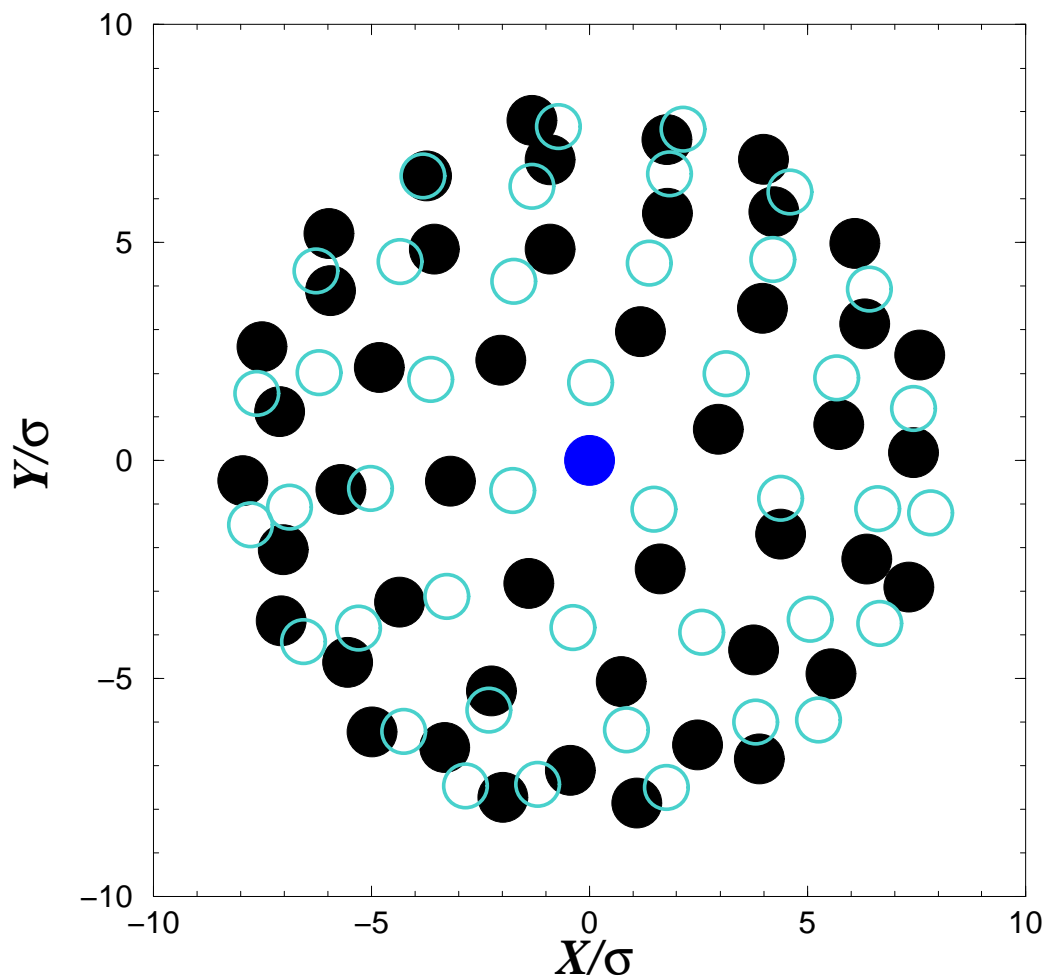
$R/a = 2.4$



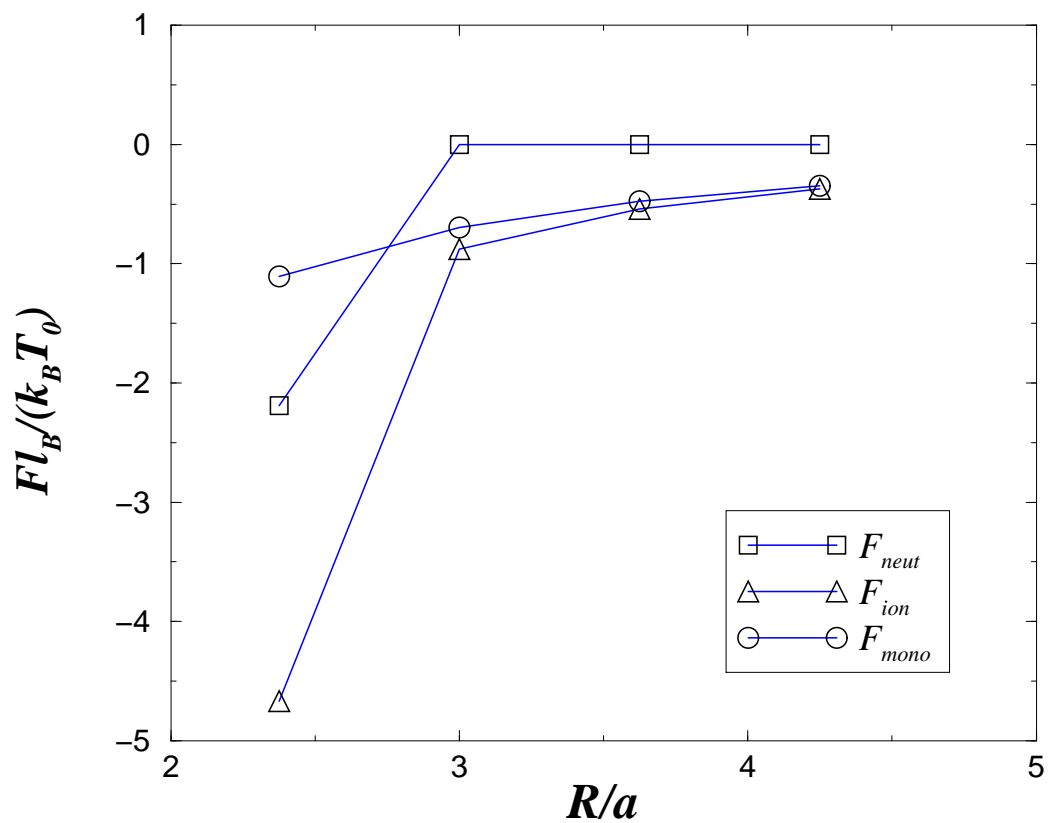
Messina et al.
Physical Review E
Figure 11 (b)

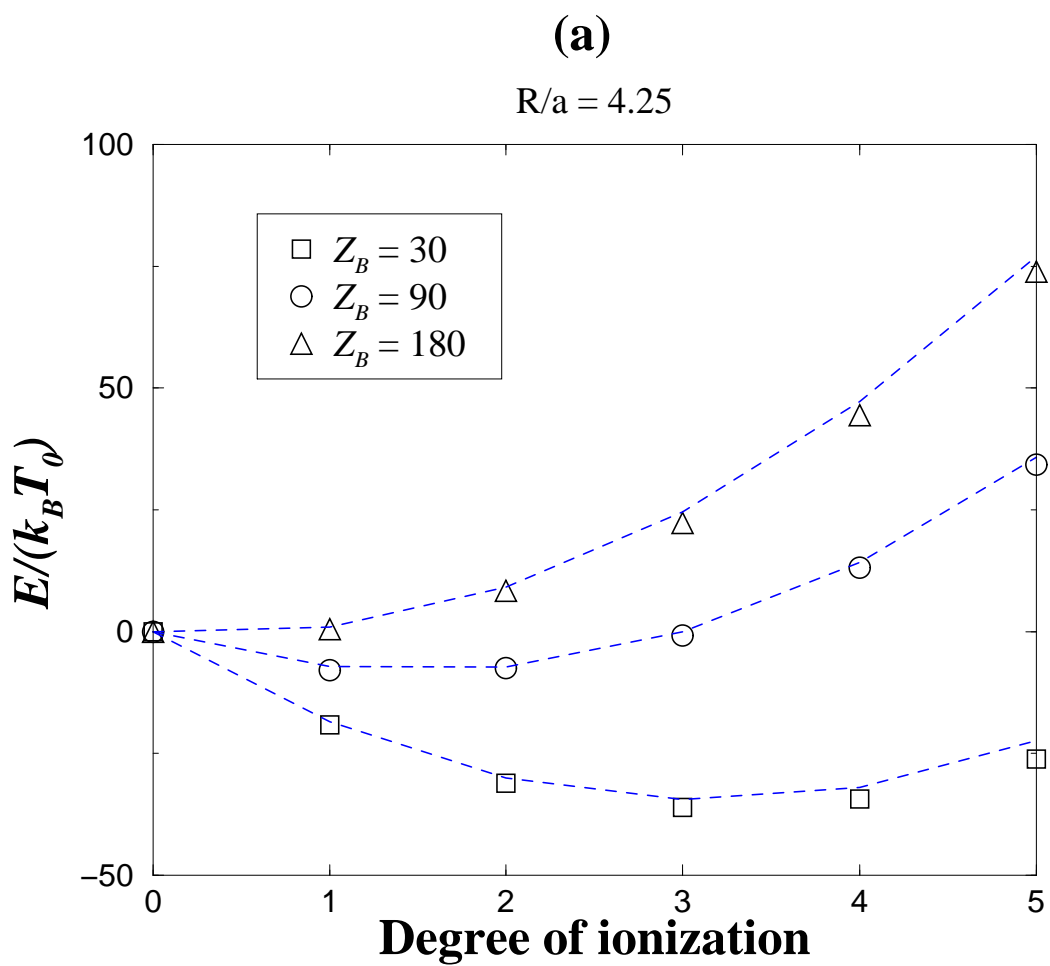


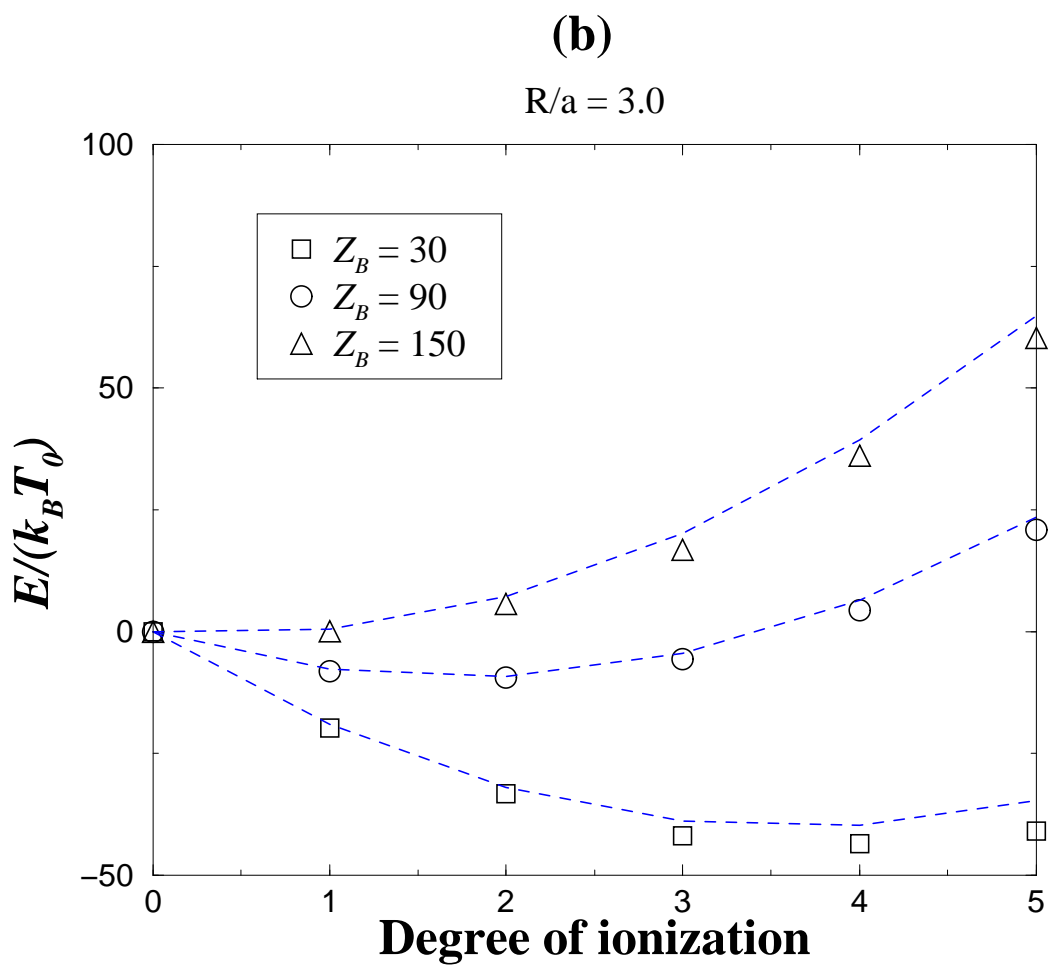
Messina et al.
Physical Review E
Figure 12



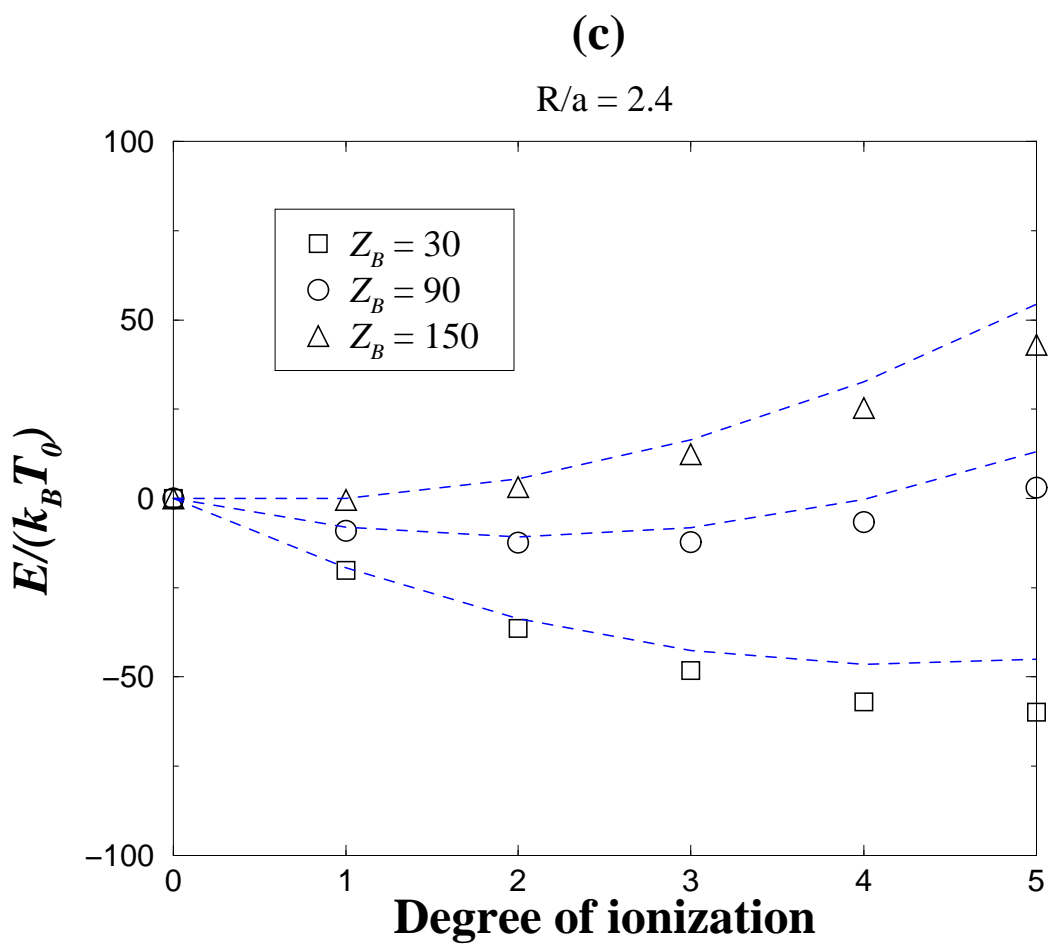
Messina et al.
Physical Review E
Figure 13



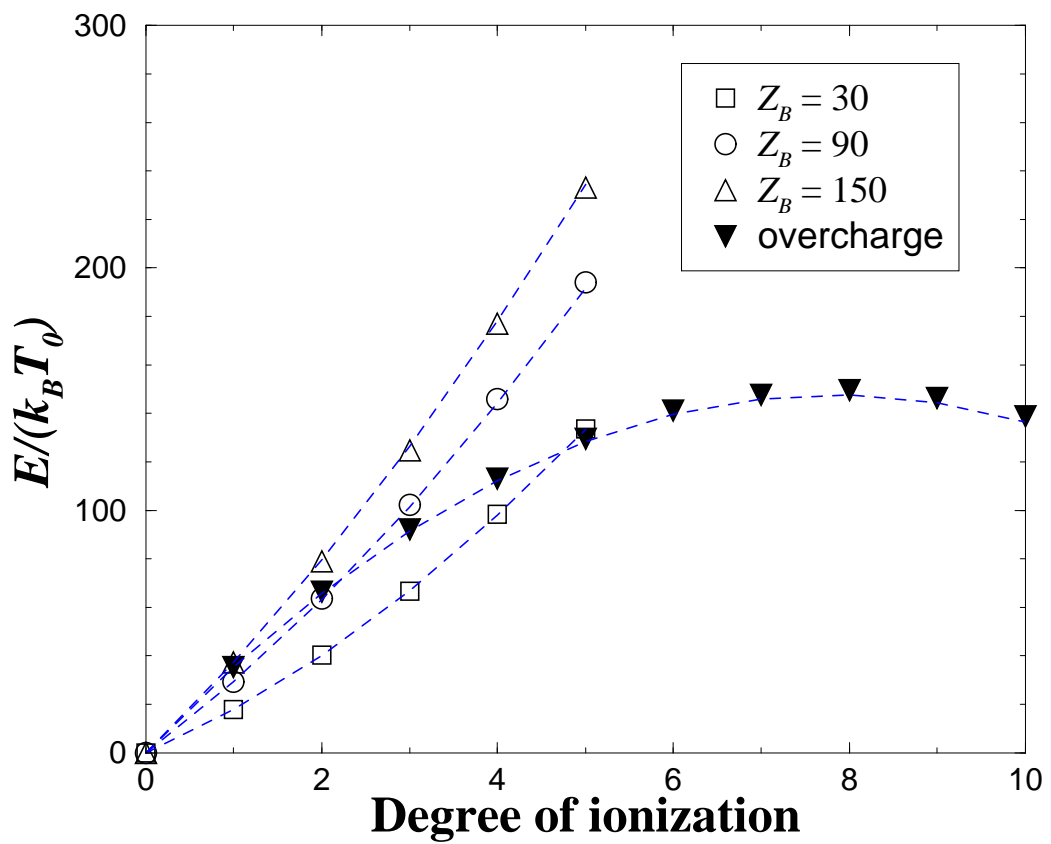




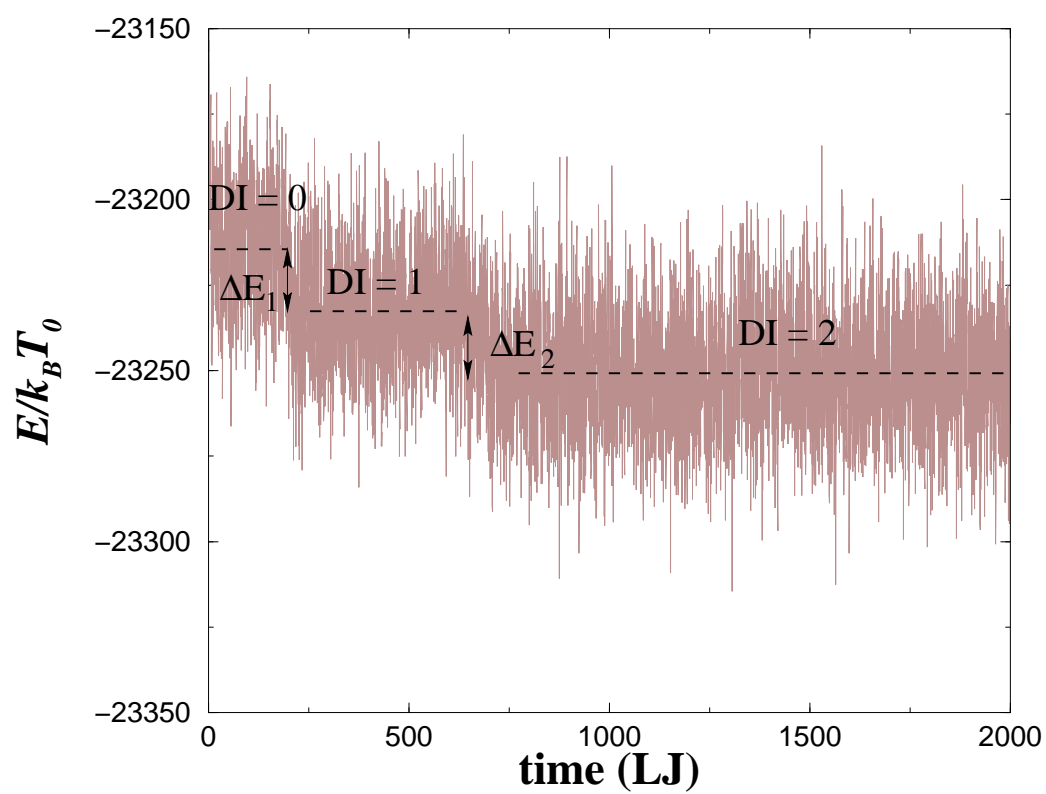
Messina et al.
Physical Review E
Figure 14 (c)



Messina et al.
Physical Review E
Figure 15



Messina et al.
Physical Review E
Figure 16



Messina et al.
Physical Review E
Figure 17

